

PAIRBENCH: ARE VISION-LANGUAGE MODELS RELIABLE AT COMPARING WHAT THEY SEE?

000
001
002
003
004
005 **Anonymous authors**
006 Paper under double-blind review
007
008
009
010

ABSTRACT

011 Understanding how effectively large vision language models (VLMs) compare vi-
012 sual inputs is crucial across numerous applications, yet this fundamental capability
013 remains insufficiently assessed. While VLMs are increasingly deployed for tasks
014 requiring comparative judgment, including automated evaluation, re-ranking, and
015 retrieval-augmented generation, no systematic framework exists to measure their
016 performance in these scenarios. We present **PAIRBENCH**, a simple framework
017 that evaluates VLMs as customizable similarity tools using widely available image
018 datasets. Our approach introduces four key metrics for reliable comparison: align-
019 ment with scores derived from human annotations, consistency across pair ordering,
020 distribution smoothness, and controllability through prompting. Our analysis re-
021 veals that no model consistently excels across all metrics, with each demonstrating
022 distinct strengths and weaknesses. Most concerning is the widespread inability
023 of VLMs to maintain symmetric similarity scores. Interestingly, we demonstrate
024 that performance on our benchmark strongly correlates with popular benchmarks
025 used for complex reasoning tasks, while providing additional insight into con-
026 trollability, smoothness and ordering. This makes **PAIRBENCH** a unique and
027 comprehensive framework to evaluate the performance of VLMs for automatic
028 evaluation, while offering an efficient predictor of model capabilities for more com-
029 plex tasks. Our evaluation code and dataset are available to the research community
030 at <https://anonymous.4open.science/r/pairbench-6C08>.

1 INTRODUCTION

031 Vision language models (VLMs) have progressed to the point of having impressive performance on
032 a wide array of tasks (Achiam et al., 2023; Laurençon et al., 2024; Reid et al., 2024; Abdin et al.,
033 2024; Wang et al., 2024c; Grattafiori et al., 2024), ranging from summarization and visual question
034 answering to image captioning and common sense reasoning (Kembhavi et al., 2016; Johnson et al.,
035 2017; Zellers et al., 2019; Lu et al., 2023; Chen et al., 2024b; Liu et al., 2025; Kazemi et al., 2024;
036 Kil et al., 2024). While human evaluation remains the gold standard for assessing model outputs,
037 it is expensive, time-consuming, and prone to inconsistency due to annotator variance (Liu et al.,
038 2019; Knox et al., 2024; Feng et al., 2024). Consequently, practitioners increasingly deploy more
039 powerful VLMs as automated evaluators across diverse applications including model assessment,
040 content ranking, and information retrieval systems (Mañas et al., 2024; Liu et al., 2024a; 2025).

041 The efficacy of VLMs in these comparative tasks fundamentally depends on their ability to function
042 as reliable similarity kernels, consistently measuring the relevance between data pairs regardless
043 of context. However, this critical capability remains insufficiently examined. Current evaluation
044 approaches either fail to isolate comparison abilities or require expensive expert validation, and
045 little to no guidance exists when selecting models for comparison-dependent tasks. As illustrated
046 in Figure 1, even widely used and highly capable commercial models like GPT-4o-1120 and
047 Gemini-1.5-Pro demonstrate concerning inconsistencies when comparing visual inputs, some-
048 times failing to follow similarity assessment instructions or producing asymmetric scores for identical
049 pairs presented in different orders, which exemplifies the extent to which evaluation of comparison
050 skills are lacking.

051 To address this gap, we introduce **PAIRBENCH**, a framework designed to evaluate VLMs as similarity
052 estimators using readily available datasets and straightforward transformation techniques. Our ap-
053 proach optimizes the signal-to-evaluation cost ratio by focusing on four essential metrics: **MMScore**

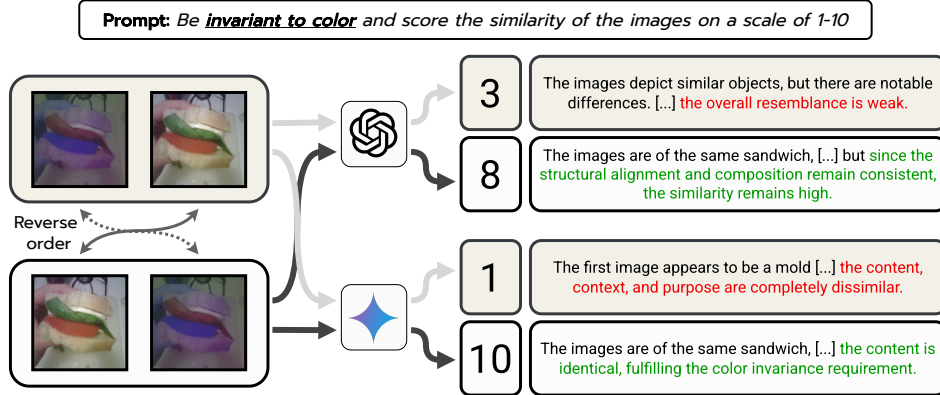


Figure 1: Image order change; prompting GPT-4o-1120 and Gemini-1.5-Pro with identical text and image prompts, differing only in image order, leads to varying predicted scores. *Auto evaluators defined by these models will yield drastically different judgments after minor changes in the prompt.* Detailed failure cases of state-of-the-art models are reported in Appendix A.

(alignment with human judgment), **ε -RelaxSym** (consistency across pair ordering), **Smoothness** (distribution of scores), and **Controllability** (response to prompt instructions). We instantiated PAIRBENCH using easily accessible datasets. Namely, ImageNet (Deng et al., 2009), MS-COCO (Lin et al., 2014), and WhatsUp (Kamath et al., 2023) seeded the evaluation suite we built. We further conducted a human study to establish ground truth similarity scores that enable direct measurement of how well model assessments align with human perception. By applying controlled transformations to create synthetic paired images with specific feature differences, PAIRBENCH enables precise examination of model biases and strengths in detecting various types of visual differences.

We carried out an extensive evaluation covering several state-of-the-art VLMs, both proprietary and open-source, multiple dataset configurations, and different prompt templates. Results reveal not only significant variations in comparison capabilities across different architectures and training approaches, but also show concerning asymmetries in how models process the same data pairs when presented in different orders, and highlight which models can be effectively controlled through prompt instructions. Remarkably, despite its simplicity, the performance on PAIRBENCH strongly correlates with results on complex reasoning benchmarks (Yue et al., 2024; Lu et al., 2023; Chen et al., 2024b; Guan et al., 2024; Liu et al., 2024b; Kembhavi et al., 2016), suggesting that many advanced tasks ultimately rely on models functioning as effective similarity kernels.

Our contributions are as follows:

- We propose **PAIRBENCH**, a framework for evaluating VLMs as similarity kernels, which does not require additional expert annotations and is cheap to instantiate.
- We further create and release¹ four instantiations of PAIRBENCH using popular datasets - ImageNet, MS-COCO, and WhatsUp - which consist of 70K data pairs for comparisons.
- We carry out a broad benchmarking of several closed- and open-source VLMs on the different configurations within our proposed dataset instantiations to show how models differ and give insight into what extent they can be trusted to act as auto evaluators on image-image and image-text data pairs.
- Lastly, we report the correlations of the results of our framework with popular benchmarks and show the ability to compare, captured by the metrics in PAIRBENCH, have predictive power of performance on several tasks and can act as a low-cost surrogate during training or validation of VLMs.

¹<https://huggingface.co/datasets/feiziaarash/pairbench>

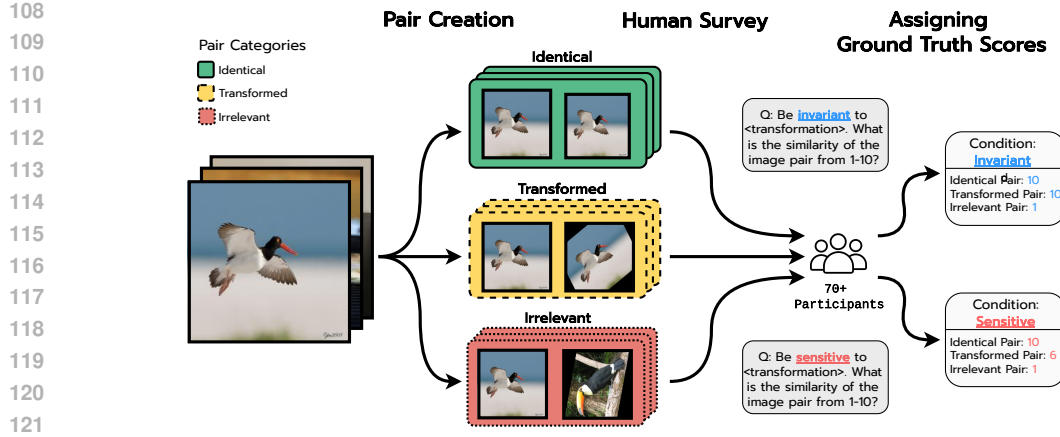


Figure 2: Dataset creation pipeline for the image-image datasets, i.e., PBcoco, PB_{IN100}, and PB_{WU-II}. Each original image is used to create three pairs of image: identical, transformed, and irrelevant. Finally, based on the human study, each pair is scores depending on the condition of the prompt.

2 PAIRBENCH

2.1 DATASET CREATION

To evaluate how well vision-language models can assess similarity under controlled transformations, we construct a dataset using the PAIRBENCH framework, illustrated in Figure 2. For each original image, we generate three types of pairs: (1) Identical pairs where the second image is a near-duplicate, (2) Transformed pairs where a specific transformation (e.g., color jitter or spatial shift) is applied, and (3) Irrelevant pairs with unrelated content. We then gather similarity judgments from over 70 human annotators under two distinct conditions: invariant, where models should ignore transformations and focus on semantic similarity, and sensitive, where models should penalize such transformations. These human ratings verify the assignment of ground-truth similarity scores: both identical and irrelevant pairs are assigned fixed values of 10 and 1, respectively, while transformed pairs receive a score of 10 under invariance and 6 under sensitivity.

The framework is instantiated across image-only datasets (COCO, IN100) and image-text datasets (WhatsUp), using five standard image transformations plus a spatial position shift known to challenge VLMs. Full construction details, including transformation splits, prompt templates used to reduce linguistic bias, and details of the human study procedure, are provided in Appendix D.

2.2 METRICS

To measure the reliability of VLMs in scoring data pairs, we define four metrics that we measure across datasets and models: *MMScore*, ε -RelaxSym, Smoothness (*SM*), and Controllability (*Cont*).

We adopt the following notation to formulate the metrics: we denote the VLM being evaluated as \mathcal{M} and the condition, which determines if the prompt instructs the model to be sensitive or invariant to a visual feature, as $C \in \{\text{sens}, \text{inv}\}$. Finally, given a dataset $\mathcal{D}_N = \{(d_1, d_2), (d_3, d_4), \dots, (d_{2N-1}, d_{2N})\}$, we denote the similarity score of a data pair $(d_i, d_j) \in \mathcal{D}_N$ returned by an VLM (\mathcal{M}) for a given condition (C) as:

$$s_{\mathcal{M}}^C(d_i, d_j) := \mathcal{M}(C, d_i, d_j),$$

where (d_i, d_j) could be an image-image or image-text pair. Note that we instruct the model to generate the output in a structured format to make sure the predicted score is parsable from the model output. If $s_{\mathcal{M}}^C(d_i, d_j)$ is valid, it would fall in the set $\mathcal{V} = [1, 10]$. However, models often do not consistently follow the details of the prompt and may produce scores not in \mathcal{V} or outputs that do not satisfy the output format, in which case we set $s_{\mathcal{M}}^C(d_i, d_j) = -1$. Finally, to evaluate a model \mathcal{M} on \mathcal{D}_N given condition C , we create and annotate the set of all its outputs as:

$$S_{\mathcal{M}}^C(\mathcal{D}_N) = \{s_{\mathcal{M}}^C(d_i, d_j) \mid (d_i, d_j) \in \mathcal{D}_N \cup \text{rev}(\mathcal{D}_N)\},$$

where $\text{rev}(\mathcal{D}_N) = \{(d_2, d_1), (d_4, d_3), \dots, (d_{2N}, d_{2N-1})\}$ are the data pairs in reverse order.

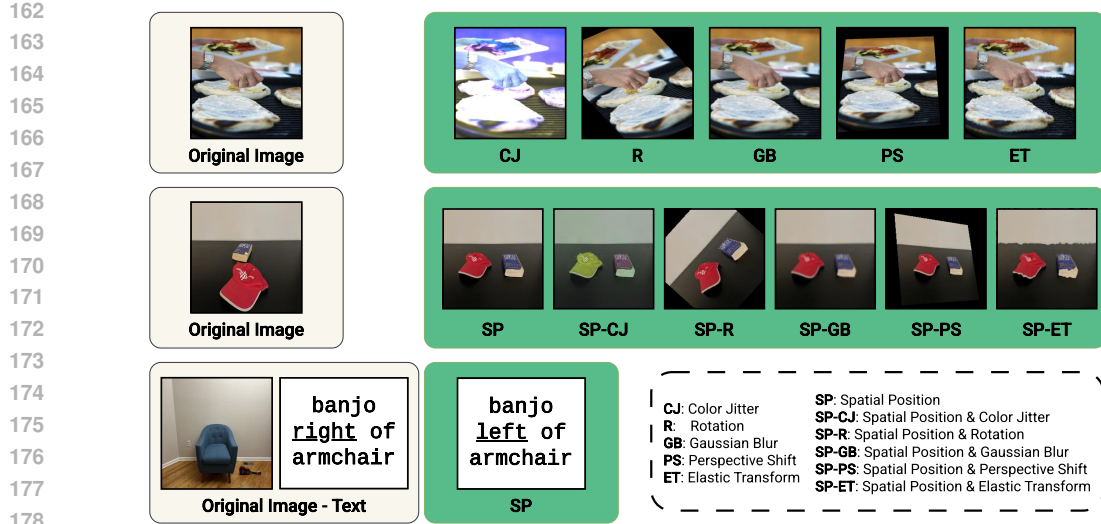


Figure 3: Examples of transformations (green boxes) applied to the original data points (gray boxes) of each subset instantiated with PAIRBENCH. The first row shows the different splits of PB_{COCO} and PB_{IN100}, the second row for PB_{WU-II}, and the third for PB_{WU-IT}.

2.2.1 MMSCORE

We first introduce *MMScore*, the main metric of PAIRBENCH, which measures the alignment between model predictions and scores derived from human assessments. To this aim, we utilize Kendall’s rank correlation coefficient (Kendall, 1938) between the predicted and the ground-truth scores. Instead of accuracy or squared error, we consider *MMScore* as we do not prompt the VLM with examples of the correct scores and hence cannot expect it to predict them directly. In other words, *MMScore* focuses on whether the VLM’s scores are consistent with the ranking of the ground-truth scores without penalizing outputs that do not exactly match in magnitude. The better a model preserves the relative ordering and variance in the ground-truth scores, the better it is able to capture that characteristic. Hence we write,

$$MMScore(\mathcal{M}, C, \mathcal{D}_N) = \text{KT}(S_{\mathcal{M}}^C(\mathcal{D}_N), GT_C(\mathcal{D}_N)),$$

where $\text{KT}(\cdot, \cdot)$ is the Kendall’s Tau and $GT_C(\cdot)$ is the ground truth of the input dataset considering the condition of C . We further explore other rank-based metrics in Appendix C.2 and observed Kendall’s Tau is the most suitable for this metric.

2.2.2 ε -RELAXSYM

The second metric we introduce aims to evaluate how consistent models are with respect to input order. This metric captures a fundamental characteristic when VLMs are used as re-rankers or automatic evaluators. Surprisingly, however, we found that most models do not satisfy exact symmetry, i.e., the equality of $sim(a, b)$ and $sim(b, a)$. We thus introduce ε -RelaxSym, which tolerates a difference of ε between the scores that should be equal. More specifically, to analyze the symmetry of VLMs on a dataset \mathcal{D}_N , we compute the ε -RelaxSym of (\mathcal{M}) on \mathcal{D}_N :

$$\varepsilon\text{-RelaxSym}(\mathcal{M}, \mathcal{D}_N) = \frac{1}{N} \sum_{(d_i, d_j) \in \mathcal{D}_N} \text{SoftEq}_{\varepsilon}(\mathcal{M}, d_i, d_j),$$

where $\text{SoftEq}_{\varepsilon}(\mathcal{M}, d_i, d_j)$ is defined as:

$$\text{SoftEq}_{\varepsilon}(\mathcal{M}, d_i, d_j) = \begin{cases} 1 & \text{if } |s_{\mathcal{M}}^C(d_i, d_j) - s_{\mathcal{M}}^C(d_j, d_i)| \leq \varepsilon, \\ 0 & \text{otherwise.} \end{cases} \quad s_{\mathcal{M}}^C(d_i, d_j), s_{\mathcal{M}}^C(d_j, d_i) \in \mathcal{V},$$

Throughout this paper, we set $\varepsilon = 1$ and provide ablation studies covering other cases in Figure 9 in the Appendix.

216 2.2.3 SMOOTHNESS
217

218 We aim to measure how smooth the kernels induced by VLMs are. For instance, a non-smooth
219 kernel would assign scores such that pairs are either exactly the same or completely different, while a
220 smoother kernel produces more nuanced distinctions. We measure smoothness via the diversity of
221 the predicted scores. Given $S_{\mathcal{M}}^C$, smoothness (SM) is computed as:

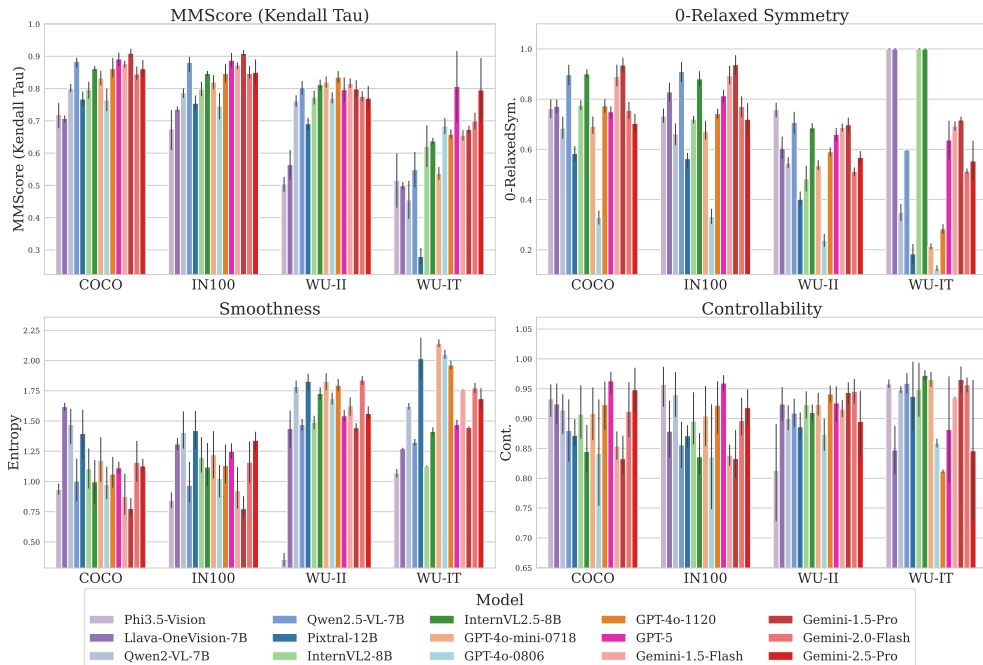
$$222 \quad 223 \quad SM(\mathcal{M}, \mathcal{D}_N, C) = Ent(\{s \mid s \in S_{\mathcal{M}}^C(\mathcal{D}_N) \text{ and } s \in \mathcal{V}\}),$$

224 where $Ent(\cdot)$ is the entropy of a set relative to its support, i.e., the set of candidate inputs.
225

226 2.2.4 CONTROLLABILITY
227

228 We measure how **responsive to instructions** models are. To do so, we define controllability based
229 on the difference in $MMScore$ between the sensitive and invariant settings. The more controllable a
230 model is, the smaller the discrepancy observed between the `sens` and `inv` settings. Hence, when
231 measuring the controllability on \mathcal{D}_N for a model \mathcal{M} is defined as

$$232 \quad 233 \quad Cont(\mathcal{M}, \mathcal{D}_N) = 1 - \frac{|MMScore(\mathcal{M}, \text{sens}, \mathcal{D}_N) - MMScore(\mathcal{M}, \text{inv}, \mathcal{D}_N)|}{\sqrt{(MMScore(\mathcal{M}, \text{sens}, \mathcal{D}_N) \times MMScore(\mathcal{M}, \text{inv}, \mathcal{D}_N))}}.$$



257 Figure 4: Best models performances on PB_{COCO}, PB_{IN100}, PB_{WU-II}, and PB_{WU-IT}. No model dominates the
258 others as a similarity kernel, hence showing the limitation of defaulting to a single model as a judge for every
259 task and dataset. Note the full symmetry of Phi-3.5-vision, LLaVA-OneVision-7B, and InternVL
260 models on PB_{WU-IT} are due to the lack of flexibility in the prompt structure to take the image anywhere but the
261 beginning.

262 3 EVALUATION RESULTS
263264 3.1 EXPERIMENTAL SETTING
265

266 We choose a comprehensive set of open- and closed-source vision-language models and evaluate
267 them using the instantiations of PAIRBENCH. From the openly available models, we evaluated
268 Chameleon-7B (Lu et al., 2024), LLaVA-OneVision-7B (Li et al., 2024), Pixtral-12B
269 (Agrawal et al., 2024), Phi-3.5-vision (Abdin et al., 2024), four model sizes (1B, 2B, 4B,

and 8B) of InternVL2 (Wang et al., 2024c), four model sizes (1B, 2B, 4B, and 8B) of InternVL2.5 (Chen et al., 2024c), two capacities (2B and 7B) of Qwen2-VL (Wang et al., 2024b), two capacities (3B and 7B) Qwen2.5-VL (Hui et al., 2024), and three versions (MolmoE-1B, Molmo-7B-O, and Molmo-7B-D) of Molmo (Deitke et al., 2024).

We also considered commercial grade models and benchmarked four versions of GPT (Achiam et al., 2023)(GPT-5, GPT-4o-0513, GPT-4o-0806, GPT-4o-1120), GPT-4o-mini-0718, and four versions of Gemini (Reid et al., 2024) (Gemini-1.5-Flash, Gemini-1.5-Pro, Gemini-2.0-Flash, Gemini-2.5-Pro). Note that we consider multiple versions of the same architecture, as opposed to using the newest/largest version, to understand better how model capacity affects each of the metrics. We provide an extended analysis of different model versions in Appendix C.3. We run all open-source models on a single NVIDIA H100 GPU using greedy sampling for inference. For closed-source models, we use API access through either OPENROUTER² or OpenAI³, applying the default inference hyperparameters provided by the respective platforms.

Also note that, since PAIRBENCH aims to evaluate VLMs as similarity kernels on image-only or text-image pairs, we do not evaluate text-only reasoning models such as OpenAI-o1 or DeepSeek-R1 (Guo et al., 2025). Further, we do not evaluate Llama3.2-11B (Grattafiori et al., 2024) as its official implementation on HuggingFace⁴ does not support Flash Attention (Dao et al., 2022) and inference was prohibitively slow. As a result, we excluded them from our final results.

Table 1: Aggregated *MMScore*, *I-RS*:1-RelaxSym, *SM*, and *Cont* over all four data splits. No model performs the best across all metrics, showing the importance of PAIRBENCH to rank models based on different abilities.

Model	<i>MMScore</i> (%)	<i>I-RS</i> (%)	<i>SM</i>	<i>Cont</i> (%)
Phi-3.5-vision	62.45	75.07	1.44	90.86
Qwen2-VL-7B	74.94	84.45	1.63	91.56
Qwen2.5-VL-7B	81.51	90.77	1.26	89.62
InternVL2-8B	77.07	74.63	1.32	91.62
InternVL2.5-8B	81.50	95.21	1.42	88.63
Pixtral-12B	68.61	74.84	1.67	88.44
GPT-4o-1120	82.86	91.50	1.52	92.28
GPT-5	83.63	96.51	1.39	93.71
Gemini-1.5-Pro	83.44	88.72	1.17	89.93
Gemini-2.5-Pro	80.80	83.67	1.44	90.7

Table 2: Spearman correlation of different metrics of PAIRBENCH with performance on other benchmarks for 23 models. *MMScore* has the highest correlation, making it the main metric.

Metric	<i>MMScore</i>	<i>I-RS</i>	<i>SM</i>	<i>Cont</i>
AI2D	79%	30%	26%	77%
HallusionBench	80%	36%	32%	67%
MMBench	77%	29%	33%	71%
MMMU	90%	34%	31%	80%
MMStar	81%	20%	33%	79%
MMVet	81%	28%	38%	68%
MathVista	73%	18%	35%	74%
OCRBench	51%	8%	37%	52%

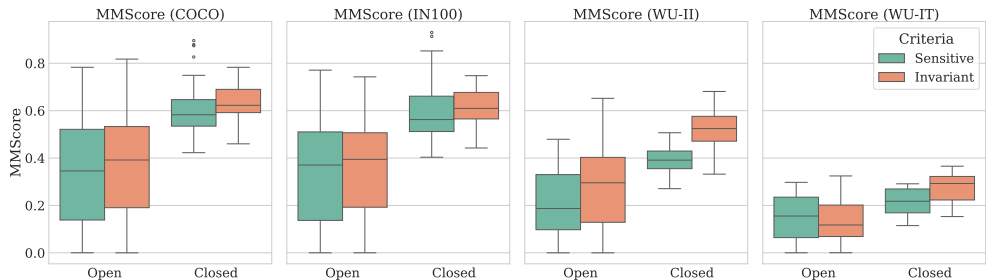


Figure 5: Closed- and open-source models perform comparable on image-text tasks. From the left to the right, the first three plots are image-image tasks, while the last is an image-text comparison task.

3.2 RESULTS

We analyze and plot the results of the best models in Figure 4 and provide an aggregated version of the metrics over all four datasets in Table 1. We aggregate different splits/datasets by taking the average

²<https://openrouter.ai/>

³<https://platform.openai.com/>

⁴<https://huggingface.co/>

324 of them to give each sub-dataset equal importance in the final number. The full set of benchmarking
 325 results of all models for PAIRBENCH on all datasets and metrics are reported in Appendix C.
 326

327 3.2.1 GENERAL OBSERVATIONS

328 As illustrated in Figure 4 and Table 1, we observe no model, whether closed- or open-source, is
 329 the best performer across all four metrics. Moreover, we further observe that for each metric,
 330 no model is the ‘best’ similarity kernel across the four different datasets either. This shows how
 331 features of the dataset and also the metrics a user might want to optimize play a crucial role in
 332 which VLM to choose as the best similarity kernel/judge. For instance, among open-source models,
 333 although InternVL2.5-8B outperforms the rest in *MMScore*, it is less controllable and smooth
 334 than Qwen2-VL-7B or LLaVA-OneVision-7B.

335 When considering PAIRBENCH’s main metric, *MMScore*, we notice that the performance of models
 336 is generally better on image-image pairs rather than image-text pairs. Furthermore, as seen in
 337 Figure 5, we observe that although open-source VLMs are roughly comparable to closed-source
 338 ones on PBWU-II, the gap between the two groups is larger in the image-image pairs. However,
 339 InternVL2.5-8B is a strong competitor to closed-source models considering all four metrics and
 340 could potentially be used as a substitute to closed-source models as a similarity kernel based on the
 341 results reported in Table 1.

342 Interestingly, we further observe a pattern regarding GPT-4o-1120, a common default judge
 343 used in the literature, and its lower cost version, GPT-4o-mini-0718; they both suffer from low
 344 1-RelaxSym when comparing image-text pairs, and the cheaper model’s *Cont* and *SM* are higher or
 345 comparable to that of the expensive one across datasets. Another fascinating result we observed was
 346 the effect the scaling effect on different metrics of PAIRBENCH for a single model family; the larger
 347 a model gets, the better it performs on *MMScore* and 1-RelaxSym. However, that does not hold for
 348 controllability and smoothness. This emphasizes the importance of PAIRBENCH in analyzing the
 349 capabilities of models, both open and closed-source, as similarity kernels to be better used as judges.
 350 We analyze and plot these results further in Appendix C and show further qualitative examples of
 351 the errors the best VLMs make in these tasks in Appendix A.

352 3.2.2 CORRELATION WITH BENCHMARKS

353 To showcase the effectiveness of our metrics and PAIRBENCH in predicting reasoning performance,
 354 we compute the Spearman correlation with respect to other popular benchmarks used in the literature.
 355 By showing correlations of our metrics with these benchmarks, we show that although the PAIR-
 356 BENCH framework introduces simple and cost-efficient methods focused on evaluating the ability to
 357 compare due to prompted VLMs, these metrics are predictive of an VLM’s performance on other
 358 tasks, and can provide an alternative for model ranking and validation during development.
 359

360 We collect all the model performances from the OPENVLM LEADERBOARD(Duan et al., 2024)
 361 and filter out the models we evaluate, resulting in all 27 (including different versions/capacities of
 362 closed- and open-source) models. By filtering out the benchmarks that have evaluation scores for
 363 all 27 models on OpenVLM, we end up with AI2D (Kembhavi et al., 2016), HallusionBench (Guan
 364 et al., 2024), MMBench (Liu et al., 2025), MMStar (Chen et al., 2024b), MMMU (Yue et al., 2024),
 365 MathVista (Lu et al., 2023), MM-Vet (Yu et al., 2023), OCRBench (Liu et al., 2024b). Each metric is
 366 aggregated for each model across all the configurations created by PAIRBENCH before computing
 367 correlations. Namely, we aggregate all features within each dataset (e.g., CJ, SP, etc.) and across all
 368 datasets (e.g., PB_COCO, PB_WU-II) and end up with an aggregate result per metric for each model.

369 As seen in Table 2, all metrics in PAIRBENCH have a high positive correlation with performances in
 370 benchmarks. More specifically, we observe that *MMScore* has strong correlations with all benchmarks,
 371 indicating that it aligns closely with overall model performance. Hence, we select it as the main
 372 metric of PAIRBENCH. Furthermore, when analyzing the correlations of PAIRBENCH’s other metrics
 373 with all benchmarks, we find that the strength of correlation reflects how much of the base skill
 374 captured by the metric is required by each benchmark. For example, HallusionBench shows the
 375 highest correlation with 1-RelaxSym, which is notable since HallusionBench focuses primarily on
 376 evaluating hallucinations in VLMs. This suggests a connection between lack of symmetry and
 377 hallucination. Another example is the highest and lowest correlation of *Cont* with MMMU and
 378 OCRBench, respectively. MMMU’s prompt mostly contain complex questions and multiple answers,
 379 whereas OCRBench features simple prompts for most questions. We hypothesize that since *Cont*

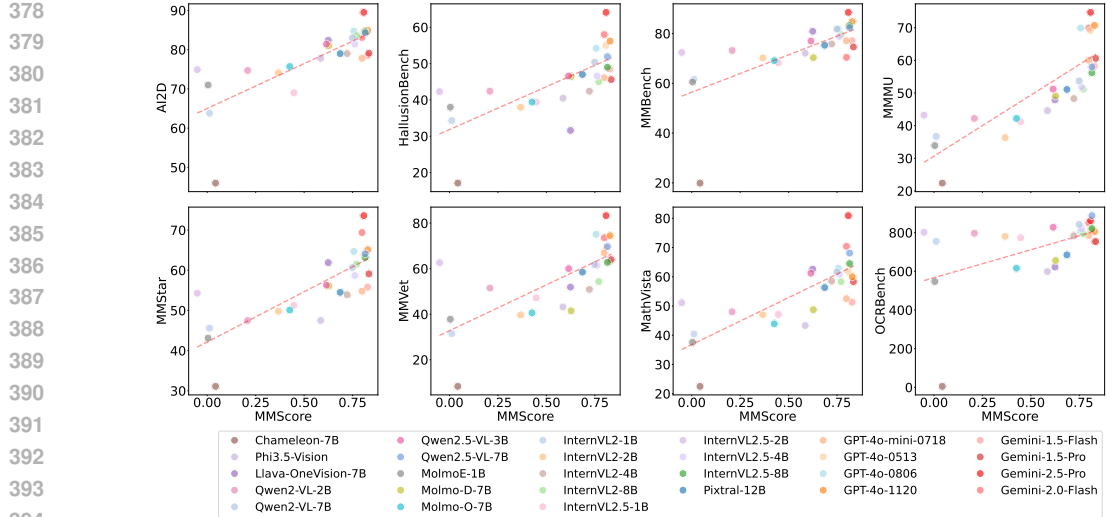


Figure 6: The main metric of PAIRBENCH, *MMScore*, strongly correlates with previous multimodal benchmarks, showcasing its predictive power of a model’s performance at a lower cost to create.

measures how well models follow the prompt, these differences explain the highest and lowest correlations observed with MMMU and OCRBench.

Note that measuring comparison skills incurs a low cost as it does not require expert-generated annotations. Our results suggest that metrics that assess these skills can serve as a low-cost surrogate of performance in various tasks: an efficient alternative to model selection. We further show scatter plots that highlight correlations in Figure 6, and more comprehensively in Figure 12 in Appendix C.

3.2.3 PROMPT SELECTION

We show the *MMScore* performance of models across datasets in Figure 7 for various prompt templates. As evident from the plots, no single prompt template consistently achieves the best performance across all models. Some models perform better with certain phrasings, while others are negatively affected by the same templates. This variation highlights the significant influence of prompt wording on model behavior. Recent work (Polo et al., 2024b) has emphasized the importance of using diverse prompts. Similarly, our randomized approach offers empirical support for that recommendation. Evaluating models with multiple prompt templates and averaging the results eliminates prompt-induced variance and leads to more reliable and fair comparisons. We recommend this strategy as a stronger and more principled standard for future benchmarking of prompted models, whether multimodal or otherwise.

4 RELATED WORK

Recent work has explored using language models as automated evaluators in NLP and vision-language domains, with approaches like GPTSCORE and G-eval (Fu et al., 2023; Liu et al., 2023) showing alignment with human preferences. However, concerns remain regarding their reliability, especially due to known limitations such as sensitivity to input order (Fang et al., 2024) and failure to infer reversible relationships (Berglund et al., 2023). In the multimodal case, work such as Zheng et al. (2023); Thakur et al. (2024); Murugadoss et al. (2024) evaluates VLMs as judges, highlighting issues of bias, prompt dependency, and limited control over evaluation criteria. Our work extends this line of research by focusing on structured pairwise comparisons, measuring not just performance alignment but also properties like symmetry, smoothness, and controllability.

While benchmarks like Chen et al. (2024a) and Awal et al. (2024) introduce ways to test comparison abilities of VLMs, we aim to provide a more systematic and transformation-aware framework. Prior work also identifies well-known blind spots in discriminative models such as CLIP, including spatial reasoning failures (Kamath et al., 2023) and neglect of logical constructs like negation (Alhamoud et al., 2025). Our goal is to support the development and evaluation of models in these areas through

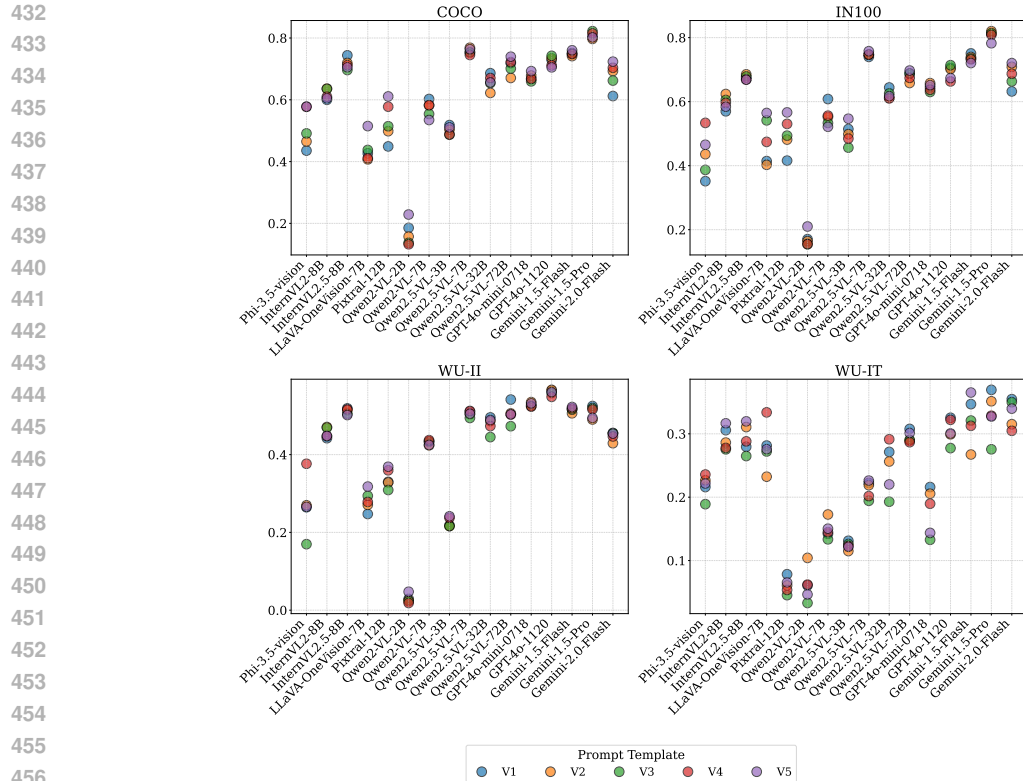


Figure 7: By using multiple prompt templates, we ensure no model is biased towards a single prompt and the mean capture the overall model performance. Above we show *MMScore*.

a carefully designed testbed. A detailed review of related evaluation benchmarks, model limitations, and pair-comparison studies is included in Appendix B.

5 CONCLUSION AND FUTURE WORK

We introduced PAIRBENCH, a framework that systematically evaluates the fundamental yet overlooked ability of VLMs to compare visual inputs, a capability critical for applications ranging from automated evaluation and re-ranking to retrieval-augmented generation. By focusing on four key metrics (alignment with human judgment, symmetry, smoothness, and controllability), PAIRBENCH provides comprehensive insights into how models process comparative information while intentionally minimizing computational requirements. This cost-efficiency addresses growing concerns around the unsustainable costs of model evaluation, which increasingly constitutes a significant portion of model development budgets (Polo et al., 2024a; Pacchiardi et al., 2024; Yuan et al., 2025).

Our extensive benchmarking revealed that no model excels across all metrics, with even leading commercial systems demonstrating concerning asymmetries when comparing identical pairs in different orders. Particularly noteworthy is our finding that performance on PAIRBENCH strongly correlates with results on complex reasoning benchmarks, suggesting that *comparison capabilities may constitute a fundamental skill* that underlies performance across diverse tasks. This insight offers a more efficient path to model selection and validation without the computational burden of exhaustive evaluations on large-scale benchmarks. As a means to further improve evaluation efficiency while accounting for sensitivity to prompting, we applied a randomized prompting strategy, rendering comparisons across models more reliable at no additional inference cost.

Looking forward, we hypothesize that tailored post-training approaches to focus on improving comparative skills and better model classes may enhance overall capabilities across diverse tasks, given the transferability our results revealed. Future research could explore architectural modifications or specialized fine-tuning techniques that optimize for these metrics, creating more reliable VLMs for critical evaluation tasks.

486 **Ethics Statement** We do not foresee any ethical issues with our work and have complied with
 487 the conference guidelines. We believe our work will aid in the better and safer usage of VLMs in
 488 practice, as we offer means to evaluate and understand model behavior prior to deployment. This
 489 can help mitigate potential risks associated with model biases and inconsistencies, leading to more
 490 reliable and transparent systems. As per language model usage, besides the evaluations we reported,
 491 we restricted ourselves to using these only to refine or rephrase handwritten parts of the manuscript
 492 to ensure correctness and clarity.

493 **Reproducibility Statement** We disclose all the details needed to carry out our evaluation such as
 494 exact prompt templates, exact model versions, and inference settings.

495 A sample of the data and example code to compute metrics are included as part of the supplementary
 496 material, and the full dataset is made anonymously available at <https://anonymous.4open.science/r/pairbench-6C08>.

500 **REFERENCES**

501 Marah Abdin, Sam Ade Jacobs, Ammar Ahmad Awan, Jyoti Aneja, Ahmed Awadallah, Hany
 502 Awadalla, Nguyen Bach, Amit Bahree, Arash Bakhtiari, Harkirat Behl, et al. Phi-3 technical report:
 503 A highly capable language model locally on your phone. *arXiv preprint arXiv:2404.14219*, 2024.

504 Josh Achiam, Steven Adler, Sandhini Agarwal, Lama Ahmad, Ilge Akkaya, Florencia Leoni Aleman,
 505 Diogo Almeida, Janko Altenschmidt, Sam Altman, Shyamal Anadkat, et al. Gpt-4 technical report.
 506 *arXiv preprint arXiv:2303.08774*, 2023.

507 Pravesh Agrawal, Szymon Antoniak, Emma Bou Hanna, Baptiste Bout, Devendra Chaplot, Jessica
 508 Chudnovsky, Diogo Costa, Baudouin De Monicault, Saurabh Garg, Theophile Gervet, et al. Pixtral
 509 12b. *arXiv preprint arXiv:2410.07073*, 2024.

510 Kumail Alhamoud, Shaden Alshammari, Yonglong Tian, Guohao Li, Philip Torr, Yoon Kim,
 511 and Marzyeh Ghassemi. Vision-language models do not understand negation. *arXiv preprint
 512 arXiv:2501.09425*, 2025.

513 Rabiul Awal, Saba Ahmadi, Le Zhang, and Aishwarya Agrawal. Vismin: Visual minimal-change
 514 understanding. *arXiv preprint arXiv:2407.16772*, 2024.

515 Lukas Berglund, Meg Tong, Max Kaufmann, Mikita Balesni, Asa Cooper Stickland, Tomasz Korbak,
 516 and Owain Evans. The reversal curse: Llms trained on "a is b" fail to learn "b is a". *arXiv preprint
 517 arXiv:2309.12288*, 2023.

518 Dongping Chen, Ruoxi Chen, Shilin Zhang, Yinuo Liu, Yaochen Wang, Huichi Zhou, Qihui Zhang,
 519 Pan Zhou, Yao Wan, and Lichao Sun. Milm-as-a-judge: Assessing multimodal llm-as-a-judge with
 520 vision-language benchmark. *arXiv preprint arXiv:2402.04788*, 2024a.

521 Lin Chen, Jinsong Li, Xiaoyi Dong, Pan Zhang, Yuhang Zang, Zehui Chen, Haodong Duan, Jiaqi
 522 Wang, Yu Qiao, Dahua Lin, et al. Are we on the right way for evaluating large vision-language
 523 models? *arXiv preprint arXiv:2403.20330*, 2024b.

524 Zhe Chen, Weiyun Wang, Yue Cao, Yangzhou Liu, Zhangwei Gao, Erfei Cui, Jinguo Zhu, Shenglong
 525 Ye, Hao Tian, Zhaoyang Liu, et al. Expanding performance boundaries of open-source multimodal
 526 models with model, data, and test-time scaling. *arXiv preprint arXiv:2412.05271*, 2024c.

527 Cheng-Han Chiang and Hung-yi Lee. Can large language models be an alternative to human
 528 evaluations? *arXiv preprint arXiv:2305.01937*, 2023.

529 Tri Dao, Daniel Y. Fu, Stefano Ermon, Atri Rudra, and Christopher Ré. FlashAttention: Fast and
 530 memory-efficient exact attention with IO-awareness. In *Advances in Neural Information Processing
 531 Systems (NeurIPS)*, 2022.

532 Matt Deitke, Christopher Clark, Sangho Lee, Rohun Tripathi, Yue Yang, Jae Sung Park, Moham-
 533 madreza Salehi, Niklas Muennighoff, Kyle Lo, Luca Soldaini, et al. Molmo and pixmo: Open
 534 weights and open data for state-of-the-art multimodal models. *arXiv preprint arXiv:2409.17146*,
 535 2024.

540 Jia Deng, Wei Dong, Richard Socher, Li-Jia Li, Kai Li, and Li Fei-Fei. Imagenet: A large-scale
 541 hierarchical image database. In *2009 IEEE conference on computer vision and pattern recognition*,
 542 pp. 248–255. Ieee, 2009.

543

544 Haodong Duan, Junming Yang, Yuxuan Qiao, Xinyu Fang, Lin Chen, Yuan Liu, Xiaoyi Dong, Yuhang
 545 Zang, Pan Zhang, Jiaqi Wang, et al. Vlmevalkit: An open-source toolkit for evaluating large
 546 multi-modality models. In *Proceedings of the 32nd ACM International Conference on Multimedia*,
 547 pp. 11198–11201, 2024.

548

549 Lizhe Fang, Yifei Wang, Khashayar Gatmiry, Lei Fang, and Yisen Wang. Rethinking invariance in
 550 in-context learning. In *ICML 2024 Workshop on Theoretical Foundations of Foundation Models*,
 551 2024.

552

553 Kehua Feng, Keyan Ding, Kede Ma, Zhihua Wang, Qiang Zhang, and Huajun Chen. Sample-efficient
 554 human evaluation of large language models via maximum discrepancy competition. *arXiv preprint*
 555 *arXiv:2404.08008*, 2024.

556

557 Jinlan Fu, See-Kiong Ng, Zhengbao Jiang, and Pengfei Liu. Gptscore: Evaluate as you desire. *arXiv*
 558 *preprint arXiv:2302.04166*, 2023.

559

560 Aaron Grattafiori, Abhimanyu Dubey, Abhinav Jauhri, Abhinav Pandey, Abhishek Kadian, Ahmad
 561 Al-Dahle, Aiesha Letman, Akhil Mathur, Alan Schelten, Alex Vaughan, Amy Yang, Angela Fan,
 562 Anirudh Goyal, Anthony Hartshorn, Aobo Yang, Archi Mitra, Archie Sravankumar, Artem Korenev,
 563 Arthur Hinsvark, Arun Rao, Aston Zhang, Aurelien Rodriguez, Austen Gregerson, Ava Spataru,
 564 Baptiste Roziere, Bethany Biron, Binh Tang, Bobbie Chern, Charlotte Caucheteux, Chaya Nayak,
 565 Chloe Bi, Chris Marra, Chris McConnell, Christian Keller, Christophe Touret, Chunyang Wu,
 566 Corinne Wong, Cristian Canton Ferrer, Cyrus Nikolaidis, Damien Allonsius, Daniel Song, Danielle
 567 Pintz, Danny Livshits, Danny Wyatt, David Esiobu, Dhruv Choudhary, Dhruv Mahajan, Diego
 568 Garcia-Olano, Diego Perino, Dieuwke Hupkes, Egor Lakomkin, Ehab AlBadawy, Elina Lobanova,
 569 Emily Dinan, Eric Michael Smith, Filip Radenovic, Francisco Guzmán, Frank Zhang, Gabriel
 570 Synnaeve, Gabrielle Lee, Georgia Lewis Anderson, Govind Thattai, Graeme Nail, Gregoire Mialon,
 571 Guan Pang, Guillem Cucurell, Hailey Nguyen, Hannah Korevaar, Hu Xu, Hugo Touvron, Iliyan
 572 Zarov, Imanol Arrieta Ibarra, Isabel Kloumann, Ishan Misra, Ivan Evtimov, Jack Zhang, Jade Copet,
 573 Jaewon Lee, Jan Geffert, Jana Vrane, Jason Park, Jay Mahadeokar, Jeet Shah, Jelmer van der Linde,
 574 Jennifer Billock, Jenny Hong, Jenya Lee, Jeremy Fu, Jianfeng Chi, Jianyu Huang, Jiawen Liu, Jie
 575 Wang, Jiecao Yu, Joanna Bitton, Joe Spisak, Jongsoo Park, Joseph Rocca, Joshua Johnstun, Joshua
 576 Saxe, Junteng Jia, Kalyan Vasuden Alwala, Karthik Prasad, Kartikeya Upasani, Kate Plawiak,
 577 Ke Li, Kenneth Heafield, Kevin Stone, Khalid El-Arini, Krithika Iyer, Kshitiz Malik, Kuenley
 578 Chiu, Kunal Bhalla, Kushal Lakhota, Lauren Rantala-Yeary, Laurens van der Maaten, Lawrence
 579 Chen, Liang Tan, Liz Jenkins, Louis Martin, Lovish Madaan, Lubo Malo, Lukas Blecher, Lukas
 580 Landzaat, Luke de Oliveira, Madeline Muzzi, Mahesh Pasupuleti, Mannat Singh, Manohar Paluri,
 581 Marcin Kardas, Maria Tsimpoukelli, Mathew Oldham, Mathieu Rita, Maya Pavlova, Melanie
 582 Kambadur, Mike Lewis, Min Si, Mitesh Kumar Singh, Mona Hassan, Naman Goyal, Narjes
 583 Torabi, Nikolay Bashlykov, Nikolay Bogoychev, Niladri Chatterji, Ning Zhang, Olivier Duchenne,
 584 Onur Çelebi, Patrick Alrassy, Pengchuan Zhang, Pengwei Li, Petar Vasic, Peter Weng, Prajjwal
 585 Bhargava, Pratik Dubal, Praveen Krishnan, Punit Singh Koura, Puxin Xu, Qing He, Qingxiao Dong,
 586 Ragavan Srinivasan, Raj Ganapathy, Ramon Calderer, Ricardo Silveira Cabral, Robert Stojnic,
 587 Roberta Raileanu, Rohan Maheswari, Rohit Girdhar, Rohit Patel, Romain Sauvestre, Ronnie
 588 Polidoro, Roshan Sumbaly, Ross Taylor, Ruan Silva, Rui Hou, Rui Wang, Saghar Hosseini, Sahana
 589 Chennabasappa, Sanjay Singh, Sean Bell, Seohyun Sonia Kim, Sergey Edunov, Shaoliang Nie,
 590 Sharan Narang, Sharath Raparth, Sheng Shen, Shengye Wan, Shruti Bhosale, Shun Zhang, Simon
 591 Vandenhende, Soumya Batra, Spencer Whitman, Sten Sootla, Stephane Collot, Suchin Gururangan,
 592 Sydney Borodinsky, Tamar Herman, Tara Fowler, Tarek Sheasha, Thomas Georgiou, Thomas
 593 Scialom, Tobias Speckbacher, Todor Mihaylov, Tong Xiao, Ujjwal Karn, Vedanuj Goswami,
 Vibhor Gupta, Vignesh Ramanathan, Viktor Kerkez, Vincent Gonguet, Virginie Do, Vish Vogeti,
 Vitor Albiero, Vladan Petrovic, Weiwei Chu, Wenhan Xiong, Wenyin Fu, Whitney Meers, Xavier
 Martinet, Xiaodong Wang, Xiaofang Wang, Xiaoqing Ellen Tan, Xide Xia, Xinfeng Xie, Xuchao
 Jia, Xuewei Wang, Yaelle Goldschlag, Yashesh Gaur, Yasmine Babaei, Yi Wen, Yiwen Song,
 Yuchen Zhang, Yue Li, Yuning Mao, Zacharie Delpierre Coudert, Zheng Yan, Zhengxing Chen, Zoe
 Papakipos, Aaditya Singh, Aayushi Srivastava, Abha Jain, Adam Kelsey, Adam Shajnfeld, Adithya

594 Gangidi, Adolfo Victoria, Ahuva Goldstand, Ajay Menon, Ajay Sharma, Alex Boesenber, Alexei
 595 Baevski, Allie Feinstein, Amanda Kallet, Amit Sangani, Amos Teo, Anam Yunus, Andrei Lupu,
 596 Andres Alvarado, Andrew Caples, Andrew Gu, Andrew Ho, Andrew Poulton, Andrew Ryan, Ankit
 597 Ramchandani, Annie Dong, Annie Franco, Anuj Goyal, Aparajita Saraf, Arkabandhu Chowdhury,
 598 Ashley Gabriel, Ashwin Bharambe, Assaf Eisenman, Azadeh Yazdan, Beau James, Ben Maurer,
 599 Benjamin Leonhardi, Bernie Huang, Beth Loyd, Beto De Paola, Bhargavi Paranjape, Bing Liu,
 600 Bo Wu, Boyu Ni, Braden Hancock, Bram Wasti, Brandon Spence, Brani Stojkovic, Brian Gamido,
 601 Britt Montalvo, Carl Parker, Carly Burton, Catalina Mejia, Ce Liu, Changhan Wang, Changkyu
 602 Kim, Chao Zhou, Chester Hu, Ching-Hsiang Chu, Chris Cai, Chris Tindal, Christoph Feichtenhofer,
 603 Cynthia Gao, Damon Civin, Dana Beaty, Daniel Kreymer, Daniel Li, David Adkins, David Xu,
 604 Davide Testuggine, Delia David, Devi Parikh, Diana Liskovich, Didem Foss, Dingkang Wang, Duc
 605 Le, Dustin Holland, Edward Dowling, Eissa Jamil, Elaine Montgomery, Eleonora Presani, Emily
 606 Hahn, Emily Wood, Eric-Tuan Le, Erik Brinkman, Esteban Arcaute, Evan Dunbar, Evan Smothers,
 607 Fei Sun, Felix Kreuk, Feng Tian, Filippos Kokkinos, Firat Ozgenel, Francesco Caggioni, Frank
 608 Kanayet, Frank Seide, Gabriela Medina Florez, Gabriella Schwarz, Gada Badeer, Georgia Swee,
 609 Gil Halpern, Grant Herman, Grigory Sizov, Guangyi, Zhang, Guna Lakshminarayanan, Hakan Inan,
 610 Hamid Shojanazeri, Han Zou, Hannah Wang, Hanwen Zha, Haroun Habeeb, Harrison Rudolph,
 611 Helen Suk, Henry Aspegen, Hunter Goldman, Hongyuan Zhan, Ibrahim Damlaj, Igor Molybog,
 612 Igor Tufanov, Ilias Leontiadis, Irina-Elena Veliche, Itai Gat, Jake Weissman, James Geboski, James
 613 Kohli, Janice Lam, Japhet Asher, Jean-Baptiste Gaya, Jeff Marcus, Jeff Tang, Jennifer Chan, Jenny
 614 Zhen, Jeremy Reizenstein, Jeremy Teboul, Jessica Zhong, Jian Jin, Jingyi Yang, Joe Cummings,
 615 Jon Carvill, Jon Shepard, Jonathan McPhie, Jonathan Torres, Josh Ginsburg, Junjie Wang, Kai
 616 Wu, Kam Hou U, Karan Saxena, Kartikay Khandelwal, Katayoun Zand, Kathy Matosich, Kaushik
 617 Veeraghavan, Kelly Michelena, Keqian Li, Kiran Jagadeesh, Kun Huang, Kunal Chawla, Kyle
 618 Huang, Lailin Chen, Lakshya Garg, Lavender A, Leandro Silva, Lee Bell, Lei Zhang, Liangpeng
 619 Guo, Licheng Yu, Liron Moshkovich, Luca Wehrstedt, Madian Khabsa, Manav Avalani, Manish
 620 Bhatt, Martynas Mankus, Matan Hasson, Matthew Lennie, Matthias Reso, Maxim Groshev, Maxim
 621 Naumov, Maya Lathi, Meghan Keneally, Miao Liu, Michael L. Seltzer, Michal Valko, Michelle
 622 Restrepo, Mihir Patel, Mik Vyatskov, Mikayel Samvelyan, Mike Clark, Mike Macey, Mike Wang,
 623 Miquel Jubert Hermoso, Mo Metanat, Mohammad Rastegari, Munish Bansal, Nandhini Santhanam,
 624 Natascha Parks, Natasha White, Navyata Bawa, Nayan Singhal, Nick Egebo, Nicolas Usunier,
 625 Nikhil Mehta, Nikolay Pavlovich Laptev, Ning Dong, Norman Cheng, Oleg Chernoguz, Olivia
 626 Hart, Omkar Salpekar, Ozlem Kalinli, Parkin Kent, Parth Parekh, Paul Saab, Pavan Balaji, Pedro
 627 Rittner, Philip Bontrager, Pierre Roux, Piotr Dollar, Polina Zvyagina, Prashant Ratanchandani,
 628 Pritish Yuvraj, Qian Liang, Rachad Alao, Rachel Rodriguez, Rafi Ayub, Raghotham Murthy,
 629 Raghu Nayani, Rahul Mitra, Rangaprabhu Parthasarathy, Raymond Li, Rebekkah Hogan, Robin
 630 Battey, Rocky Wang, Russ Howes, Ruty Rinott, Sachin Mehta, Sachin Siby, Sai Jayesh Bondu,
 631 Samyak Datta, Sara Chugh, Sara Hunt, Sargun Dhillon, Sasha Sidorov, Satadru Pan, Saurabh
 632 Mahajan, Saurabh Verma, Seiji Yamamoto, Sharadh Ramaswamy, Shaun Lindsay, Shaun Lindsay,
 633 Sheng Feng, Shenghao Lin, Shengxin Cindy Zha, Shishir Patil, Shiva Shankar, Shuqiang Zhang,
 634 Shuqiang Zhang, Sinong Wang, Sneha Agarwal, Soji Sajuyigbe, Soumith Chintala, Stephanie
 635 Max, Stephen Chen, Steve Kehoe, Steve Satterfield, Sudarshan Govindaprasad, Sumit Gupta,
 636 Summer Deng, Sungmin Cho, Sunny Virk, Suraj Subramanian, Sy Choudhury, Sydney Goldman,
 637 Tal Remez, Tamar Glaser, Tamara Best, Thilo Koehler, Thomas Robinson, Tianhe Li, Tianjun
 638 Zhang, Tim Matthews, Timothy Chou, Tzook Shaked, Varun Vontimitta, Victoria Ajayi, Victoria
 639 Montanez, Vijai Mohan, Vinay Satish Kumar, Vishal Mangla, Vlad Ionescu, Vlad Poenaru,
 640 Vlad Tiberiu Mihailescu, Vladimir Ivanov, Wei Li, Wencheng Wang, Wenwen Jiang, Wes Bouaziz,
 641 Will Constable, Xiaocheng Tang, Xiaoqian Wu, Xiaolan Wang, Xilun Wu, Xinbo Gao, Yaniv
 Kleinman, Yanjun Chen, Ye Hu, Ye Jia, Ye Qi, Yenda Li, Yilin Zhang, Ying Zhang, Yossi Adi,
 642 Youngjin Nam, Yu, Wang, Yu Zhao, Yuchen Hao, Yundi Qian, Yunlu Li, Yuzi He, Zach Rait,
 643 Zachary DeVito, Zef Rosnbrick, Zhaoduo Wen, Zhenyu Yang, Zhiwei Zhao, and Zhiyu Ma. The
 644 llama 3 herd of models, 2024. URL <https://arxiv.org/abs/2407.21783>.
 645 Tianrui Guan, Fuxiao Liu, Xiyang Wu, Ruiqi Xian, Zongxia Li, Xiaoyu Liu, Xijun Wang, Lichang
 646 Chen, Furong Huang, Yaser Yacoob, et al. Hallusionbench: an advanced diagnostic suite for entan-
 647 gled language hallucination and visual illusion in large vision-language models. In *Proceedings of
 648 the IEEE/CVF Conference on Computer Vision and Pattern Recognition*, pp. 14375–14385, 2024.
 649 Daya Guo, Dejian Yang, Haowei Zhang, Junxiao Song, Ruoyu Zhang, Runxin Xu, Qihao Zhu,
 650 Shirong Ma, Peiyi Wang, Xiao Bi, et al. Deepseek-r1: Incentivizing reasoning capability in llms

648 via reinforcement learning. *arXiv preprint arXiv:2501.12948*, 2025.
649

650 Andrew F Hayes and Klaus Krippendorff. Answering the call for a standard reliability measure for
651 coding data. *Communication methods and measures*, 1(1):77–89, 2007.

652 Yushi Hu, Benlin Liu, Jungo Kasai, Yizhong Wang, Mari Ostendorf, Ranjay Krishna, and Noah A
653 Smith. Tifa: Accurate and interpretable text-to-image faithfulness evaluation with question
654 answering. In *Proceedings of the IEEE/CVF International Conference on Computer Vision*, pp.
655 20406–20417, 2023.

656 Binyuan Hui, Jian Yang, Zeyu Cui, Jiaxi Yang, Dayiheng Liu, Lei Zhang, Tianyu Liu, Jiajun Zhang,
657 Bowen Yu, Keming Lu, et al. Qwen2. 5-coder technical report. *arXiv preprint arXiv:2409.12186*,
658 2024.

659 Justin Johnson, Bharath Hariharan, Laurens Van Der Maaten, Li Fei-Fei, C Lawrence Zitnick, and
660 Ross Girshick. Clevr: A diagnostic dataset for compositional language and elementary visual
661 reasoning. In *Proceedings of the IEEE conference on computer vision and pattern recognition*, pp.
662 2901–2910, 2017.

663 Amita Kamath, Jack Hessel, and Kai-Wei Chang. What's" up" with vision-language models?
664 investigating their struggle with spatial reasoning. *arXiv preprint arXiv:2310.19785*, 2023.

665 Mehran Kazemi, Nishanth Dikkala, Ankit Anand, Petar Devic, Ishita Dasgupta, Fangyu Liu, Bahare
666 Fatemi, Pranjal Awasthi, Sreenivas Gollapudi, Dee Guo, et al. Remi: A dataset for reasoning with
667 multiple images. *Advances in Neural Information Processing Systems*, 37:60088–60109, 2024.

668 Aniruddha Kembhavi, Mike Salvato, Eric Kolve, Minjoon Seo, Hannaneh Hajishirzi, and Ali Farhadi.
669 A diagram is worth a dozen images. In *Computer Vision–ECCV 2016: 14th European Conference,
670 Amsterdam, The Netherlands, October 11–14, 2016, Proceedings, Part IV 14*, pp. 235–251.
671 Springer, 2016.

672 Maurice G Kendall. A new measure of rank correlation. *Biometrika*, 30(1-2):81–93, 1938.

673 Jihyung Kil, Zheda Mai, Justin Lee, Arpita Chowdhury, Zihe Wang, Kerrie Cheng, Lemeng Wang,
674 Ye Liu, and Wei-Lun Harry Chao. Mllm-compbench: A comparative reasoning benchmark for
675 multimodal llms. *Advances in Neural Information Processing Systems*, 37:28798–28827, 2024.

676 W. Bradley Knox, Stephane Hatgis-Kessell, Serena Booth, Scott Niekuum, Peter Stone, and Alessan-
677 dro G Allievi. Models of human preference for learning reward functions. *Transactions on Machine
678 Learning Research*, 2024. ISSN 2835-8856. URL <https://openreview.net/forum?id=hpKJkVoThY>.

679 Hugo Laurençon, Léo Tronchon, Matthieu Cord, and Victor Sanh. What matters when building
680 vision-language models? *arXiv preprint arXiv:2405.02246*, 2024.

681 Bo Li, Yuanhan Zhang, Dong Guo, Renrui Zhang, Feng Li, Hao Zhang, Kaichen Zhang, Peiyuan
682 Zhang, Yanwei Li, Ziwei Liu, et al. Llava-onevision: Easy visual task transfer. *arXiv preprint
683 arXiv:2408.03326*, 2024.

684 Tsung-Yi Lin, Michael Maire, Serge Belongie, James Hays, Pietro Perona, Deva Ramanan, Piotr
685 Dollár, and C Lawrence Zitnick. Microsoft coco: Common objects in context. In *Computer Vision–
686 ECCV 2014: 13th European Conference, Zurich, Switzerland, September 6–12, 2014, Proceedings,
687 Part V 13*, pp. 740–755. Springer, 2014.

688 Fan Liu, Zhiyong Cheng, Changchang Sun, Yinglong Wang, Liqiang Nie, and Mohan Kankanhalli.
689 User diverse preference modeling by multimodal attentive metric learning. In *Proceedings of the
690 27th ACM international conference on multimedia*, pp. 1526–1534, 2019.

691 Haotian Liu, Chunyuan Li, Qingyang Wu, and Yong Jae Lee. Visual instruction tuning. *Advances in
692 neural information processing systems*, 36, 2024a.

693 Yang Liu, Dan Iter, Yichong Xu, Shuohang Wang, Ruochen Xu, and Chenguang Zhu. G-eval: Nlg
694 evaluation using gpt-4 with better human alignment. In *Proceedings of the 2023 Conference on
695 Empirical Methods in Natural Language Processing*, pp. 2511–2522, 2023.

702 Yuan Liu, Haodong Duan, Yuanhan Zhang, Bo Li, Songyang Zhang, Wangbo Zhao, Yike Yuan, Jiaqi
 703 Wang, Conghui He, Ziwei Liu, et al. Mmbench: Is your multi-modal model an all-around player?
 704 In *European conference on computer vision*, pp. 216–233. Springer, 2025.

705 Yuliang Liu, Zhang Li, Mingxin Huang, Biao Yang, Wenwen Yu, Chunyuan Li, Xu-Cheng Yin,
 706 Cheng-Lin Liu, Lianwen Jin, and Xiang Bai. Ocrbench: on the hidden mystery of ocr in large
 707 multimodal models. *Science China Information Sciences*, 67(12):220102, 2024b.

708 Pan Lu, Hritik Bansal, Tony Xia, Jiacheng Liu, Chunyuan Li, Hannaneh Hajishirzi, Hao Cheng,
 709 Kai-Wei Chang, Michel Galley, and Jianfeng Gao. Mathvista: Evaluating mathematical reasoning
 710 of foundation models in visual contexts. *arXiv preprint arXiv:2310.02255*, 2023.

711 Pan Lu, Baolin Peng, Hao Cheng, Michel Galley, Kai-Wei Chang, Ying Nian Wu, Song-Chun Zhu,
 712 and Jianfeng Gao. Chameleon: Plug-and-play compositional reasoning with large language models.
 713 *Advances in Neural Information Processing Systems*, 36, 2024.

714 Oscar Mañas, Benno Krojer, and Aishwarya Agrawal. Improving automatic vqa evaluation using large
 715 language models. In *Proceedings of the AAAI Conference on Artificial Intelligence*, volume 38, pp.
 716 4171–4179, 2024.

717 Bhuvanashree Murugadoss, Christian Poelitz, Ian Drosos, Vu Le, Nick McKenna, Carina Suzana
 718 Negreanu, Chris Parnin, and Advait Sarkar. Evaluating the evaluator: Measuring llms’ adherence
 719 to task evaluation instructions. *arXiv preprint arXiv:2408.08781*, 2024.

720 Yassine Ouali, Adrian Bulat, Alexandros Xenos, Anestis Zaganidis, Ioannis Maniadis Metaxas,
 721 Georgios Tzimiropoulos, and Brais Martinez. Discriminative fine-tuning of lvlms. *arXiv preprint
 722 arXiv:2412.04378*, 2024.

723 Lorenzo Pacchiardi, Lucy G Cheke, and José Hernández-Orallo. 100 instances is all you need:
 724 predicting the success of a new llm on unseen data by testing on a few instances. *arXiv preprint
 725 arXiv:2409.03563*, 2024.

726 Felipe Maia Polo, Lucas Weber, Leshem Choshen, Yuekai Sun, Gongjun Xu, and Mikhail Yurochkin.
 727 tinybenchmarks: evaluating LLMs with fewer examples. In *Forty-first International Conference on
 728 Machine Learning*, 2024a. URL <https://openreview.net/forum?id=qAml3FpfhG>.

729 Felipe Maia Polo, Ronald Xu, Lucas Weber, Mírian Silva, Onkar Bhardwaj, Leshem
 730 Choshen, Allysson Flavio Melo de Oliveira, Yuekai Sun, and Mikhail Yurochkin. Ef-
 731 ficient multi-prompt evaluation of llms. In A. Globerson, L. Mackey, D. Bel-
 732 grave, A. Fan, U. Paquet, J. Tomczak, and C. Zhang (eds.), *Advances in Neural In-
 733 formation Processing Systems*, volume 37, pp. 22483–22512. Curran Associates, Inc.,
 734 2024b. URL https://proceedings.neurips.cc/paper_files/paper/2024/file/28236482f64a72eec43706b6f3a6c511-Paper-Conference.pdf.

735 Alec Radford, Jong Wook Kim, Chris Hallacy, Aditya Ramesh, Gabriel Goh, Sandhini Agarwal,
 736 Girish Sastry, Amanda Askell, Pamela Mishkin, Jack Clark, et al. Learning transferable visual
 737 models from natural language supervision. In *International conference on machine learning*, pp.
 738 8748–8763. PMLR, 2021.

739 Machel Reid, Nikolay Savinov, Denis Teplyashin, Dmitry Lepikhin, Timothy Lillicrap, Jean-baptiste
 740 Alayrac, Radu Soricut, Angeliki Lazaridou, Orhan Firat, Julian Schrittweiser, et al. Gemini
 741 1.5: Unlocking multimodal understanding across millions of tokens of context. *arXiv preprint
 742 arXiv:2403.05530*, 2024.

743 Dylan Sam, Devin Willmott, Joao D Semedo, and J Zico Kolter. Finetuning clip to reason about
 744 pairwise differences. *arXiv preprint arXiv:2409.09721*, 2024.

745 Shreya Shankar, JD Zamfirescu-Pereira, Björn Hartmann, Aditya G Parameswaran, and Ian Arawjo.
 746 Who validates the validators? aligning llm-assisted evaluation of llm outputs with human prefer-
 747 ences. *arXiv preprint arXiv:2404.12272*, 2024.

748 Aman Singh Thakur, Kartik Choudhary, Venkat Srinik Ramayapally, Sankaran Vaidyanathan, and
 749 Diewuke Hupkes. Judging the judges: Evaluating alignment and vulnerabilities in llms-as-judges.
 750 *arXiv preprint arXiv:2406.12624*, 2024.

756 Jiayu Wang, Yifei Ming, Zhenmei Shi, Vibhav Vineet, Xin Wang, Yixuan Li, and Neel Joshi. Is a
 757 picture worth a thousand words? delving into spatial reasoning for vision language models. *arXiv*
 758 *preprint arXiv:2406.14852*, 2024a.

759
 760 Peng Wang, Shuai Bai, Sinan Tan, Shijie Wang, Zhihao Fan, Jinze Bai, Keqin Chen, Xuejing Liu,
 761 Jialin Wang, Wenbin Ge, et al. Qwen2-vl: Enhancing vision-language model's perception of the
 762 world at any resolution. *arXiv preprint arXiv:2409.12191*, 2024b.

763 Weiyun Wang, Zhe Chen, Wenhui Wang, Yue Cao, Yangzhou Liu, Zhangwei Gao, Jinguo Zhu,
 764 Xizhou Zhu, Lewei Lu, Yu Qiao, et al. Enhancing the reasoning ability of multimodal large
 765 language models via mixed preference optimization. *arXiv preprint arXiv:2411.10442*, 2024c.

766
 767 Olivia Wiles, Cheolhong Zhang, Isabela Albuquerque, Ivana Kajic, S Wang, Emanuele Bugliarello,
 768 Yasumasa Onoe, Pinelopi Papalampidi, Ira Ktena, C Knutson, et al. Revisiting text-to-image
 769 evaluation with gecko: On metrics, prompts, and human ratings. *arXiv preprint arXiv:2404.16820*,
 770 2024.

771 Weihsiao Yu, Zhengyuan Yang, Linjie Li, Jianfeng Wang, Kevin Lin, Zicheng Liu, Xinchao Wang,
 772 and Lijuan Wang. Mm-vet: Evaluating large multimodal models for integrated capabilities. *arXiv*
 773 *preprint arXiv:2308.02490*, 2023.

774 Peiwen Yuan, Yueqi Zhang, Shaoxiong Feng, Yiwei Li, Xinglin Wang, Jiayi Shi, Chuyi Tan, Boyuan
 775 Pan, Yao Hu, and Kan Li. Beyond one-size-fits-all: Tailored benchmarks for efficient evaluation.
 776 *arXiv preprint arXiv:2502.13576*, 2025.

777
 778 Xiang Yue, Yuansheng Ni, Kai Zhang, Tianyu Zheng, Ruochi Liu, Ge Zhang, Samuel Stevens, Dongfu
 779 Jiang, Weiming Ren, Yuxuan Sun, et al. Mmmu: A massive multi-discipline multimodal under-
 780 standing and reasoning benchmark for expert agi. In *Proceedings of the IEEE/CVF Conference on*
 781 *Computer Vision and Pattern Recognition*, pp. 9556–9567, 2024.

782 Mert Yuksekgonul, Federico Bianchi, Pratyusha Kalluri, Dan Jurafsky, and James Zou. When and
 783 why vision-language models behave like bags-of-words, and what to do about it? In *The Eleventh*
 784 *International Conference on Learning Representations*, 2023. URL <https://openreview.net/forum?id=KRLUvxh8uaX>.

785
 786 Rowan Zellers, Yonatan Bisk, Ali Farhadi, and Yejin Choi. From recognition to cognition: Visual
 787 commonsense reasoning. In *Proceedings of the IEEE/CVF conference on computer vision and*
 788 *pattern recognition*, pp. 6720–6731, 2019.

789
 790 Lianmin Zheng, Wei-Lin Chiang, Ying Sheng, Siyuan Zhuang, Zhanghao Wu, Yonghao Zhuang,
 791 Zi Lin, Zhuohan Li, Dacheng Li, Eric Xing, et al. Judging llm-as-a-judge with mt-bench and
 792 chatbot arena. *Advances in Neural Information Processing Systems*, 36:46595–46623, 2023.

793
 794
 795
 796
 797
 798
 799
 800
 801
 802
 803
 804
 805
 806
 807
 808
 809

Table of Contents – Appendix

	Page
A. Error Analysis	17
A.1 Gemini Model	17
A.2 GPT4o Model	18
A.3 InternVL2.5 Model	18
A.4 Pixtral Model	19
A.5 Qwen2-VL Model	20
A.6 Phi3.5 Model	21
B. Extended Related Work	22
C. Full Results	23
C.1 All ϵ -RelaxSym for Different ϵ	23
C.2 Variations of MMScore Formulation	23
C.3 Different Versions of Same Model	25
C.4 Correlations	25
C.5 Encoders vs VLMs	25
C.6 Prompt Diversity Analysis	28
D. PairBench Details	32
D.1 Dataset Creation	32
D.2 Human Study for Ground Truth Scores	34
D.3 Prompt Templates for Different PairBench Datasets	36
E. LLM Usage	38

918 A.2 GPT4O MODEL

919

920 Below is an error example of GPT-4o-1120 on a data-pair from PB_{COCO} with color jittering (CJ).

921

922

923

924

GPT-4o-1120 Evaluation Instructions**User prompt:** Evaluate the similarity of the images based on the following conditions:

- *Be invariant to color jittering while evaluating images. Even if one image has been modified with random color changes (e.g., brightness or contrast adjustments), the similarity score should remain high. If the images are different, the similarity score should decrease regardless of the jittering.*

The score should take into account how well the images align with these conditions, as well as their overall resemblance. Even if the images are identical but fail to meet the conditions, they should still receive a higher score than completely different images.

Provide a score from 1 to 10, where 1 indicates no similarity and 10 indicates identical images that fully satisfy the conditions.

Respond only in this format:

Score: <1-10>

Reason: <reason for score>

Nothing else should be included. What score would you give? "data1" "data2"

939

940

GPT-4o-1120 Response - Original Order**Model response:**

Score: 8

Reason: The images are of the same sandwich, with similar shapes and arrangements of the bread, tomato, mozzarella, and basil. The second image has substantial color jittering, but since the structural alignment and composition remain consistent, the similarity remains high.

GPT-4o-1120 Response - Reversed Order**Model response:**

Score: 3

Reason: The images depict similar objects, presumably a sandwich with layers, but there are notable differences. The first image appears distorted with altered coloration, and while it shares structural similarities with the second image, the overall resemblance is weak.

968

969

A.3 INTERNVL2.5 MODEL

970

971

Below is an error example of InternVL2.5-8B on a data-pair from PB_{COCO} with that are irrelevant to each other.

972
973
974
975
976
977
978
979
980
981
982
983
984
985
986
987
988
989
990
991**InternVL2.5-8B Evaluation Instructions**

User prompt: Evaluate the similarity of the images based on the following conditions: - *Be invariant to Gaussian blurs while evaluating images. For example, even if both images are the exact same, even if one is more blurred compared to the other, the similarity score should remain high. If the images are different, the similarity score should decrease regardless of how blurred they are.* The score should take into account how well the images align with these conditions, as well as their overall resemblance. Even if the images are identical but fail to meet the conditions, they should still receive a higher score than completely different images.

Provide a score from 1 to 10, where 1 indicates no similarity and 10 indicates identical images that fully satisfy the conditions. Respond only in this format:

Score: <1-10>

Reason: <reason for score>

Nothing else should be included. What score would you give? “data1” “data2”

992
993
994
995
996
997
998
999
1000**InternVL2.5-8B - Original Order****Model response:**

Score: 7

Reason: The images are similar in content, featuring parrots, but they are not identical. The first image is a close-up of a spider web on a wooden surface, while the second image shows two parrots on a ledge. The parrots are the main subjects in the second image, and the first image has a different focus and subject matter. The images do not meet the condition of being identical, but they share some visual elements like color and subject type.

InternVL2.5-8B - Reverse Order**Model response:**

Score: 1

Reason: The images are completely different in terms of content, subject matter, and context. The first image features colorful parrots, while the second image shows a wooden door with a spider web. There is no similarity in terms of subject, color, or composition.

1017
1018
1019
1020
1021
1022
1023
1024
1025**A.4 PIXTRAL MODEL**

Below is an error example of Pixtral-12B on a data-pair from PBcocowith rotation (R).

1026

1027

1028

1029

1030

1031

1032

1033

1034

1035

1036

1037

1038

1039

1040

1041

1042

1043

1044

1045

1046

1047

1048

1049

1050

1051

1052

1053

1054

1055

1056

1057

1058

1059

1060

1061

1062

1063

1064

1065

1066

1067

1068

1069

1070

1071

1072

1073

1074

1075

1076

1077

1078

1079

Pixtral-12B Evaluation Instructions

User prompt: Rate the similarity of these images on a scale of 1 to 10 while considering the following condition:

- Be invariant to rotations while evaluating images. For example, if one image is a rotated version of the other, the similarity score should remain high. If the images are different, the similarity score should decrease regardless of their orientation.

The score should account for both how well the images satisfy the conditions and their overall resemblance. If the images are identical but do not meet the conditions, they should still score higher than unrelated images.

Your response must follow this exact format:

Score: <1-10>

Reason: <reason for score>

Provide nothing else. What's your score? "data1" "data2"

Pixtral-12B Response - Original Order**Model response:**

Score: 8

Reason: The images depict similar scenes of people interacting with birds in natural settings. The first image features a group of people sitting on rocks with birds nearby, while the second image has a person extending their hand towards a bird in a mountainous area. Despite slight differences in the environment and specific actions, the overall theme and presence of birds and human interaction score high.

Pixtral-12B Response - Reversed Order**Model response:**

Score: 2

Reason: The images depict completely different scenes and subjects, with no recognizable similarity between them. One image shows a bird and people in a rocky area, while the other does not bear any resemblance to it.

A.5 QWEN2-VL MODEL

Below is an error example of Qwen2-VL-7B on a data-pair from PBcoco with gaussian blur (GB).

1080

1081

1082

1083

1084

1085

1086

1087

1088

1089

1090

1091

1092

1093

1094

1095

1096

1097

1098

1099

1100

1101

1102

1103

1104

1105

1106

1107

1108

1109

1110

1111

1112

1113

1114

1115

1116

1117

1118

1119

1120

1121

1122

1123

1124

1125

1126

1127

1128

1129

1130

1131

1132

1133

Qwen2-VL-7B Evaluation Instructions

User prompt: As a similarity evaluator, your responsibility is to assess the similarity of the given images while considering these conditions: - *Be sensitive to Gaussian blurs while evaluating images. For example, if both images are the same except one is a blurred version of the other, the similarity score should decrease. If the images are the same and have the same exact sharpness, the similarity score should remain high.*

The similarity score should reflect both how well the images align with the conditions and their overall resemblance. Images that are identical but do not meet the conditions should receive a moderate score, while completely unrelated images should receive the lowest score. Provide your score on a scale of 1 to 10, with 10 being identical images that fully meet the conditions. Ensure your response is in the following format:

Score: <1-10>

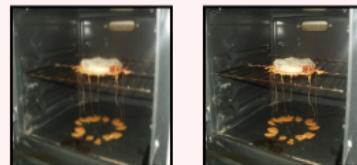
Reason: <reason for score>

Provide nothing else. What is your score? “data1” “data2”

Qwen2-VL-7B - Original Order**Model response:**

Score: 6

Reason: The images are very similar, with the second image being a slightly blurred version of the first. However, they do not fully meet the conditions as the images are not identical and the blurring is not perfect.

Qwen2-VL-7B - Reverse Order**Model response:**

Score: 9

Reason: The images are nearly identical, with only a slight difference in the sharpness of the objects. The overall resemblance is high, and the conditions are met.

A.6 PHI3.5 MODEL

Below is an error example of Phi-3.5-vision on a data-pair from PB_COCO with elastic transform (ET).

1134

1135

1136

1137

1138

1139

1140

1141

1142

1143

1144

1145

1146

1147

1148

1149

1150

1151

1152

1153

1154

1155

1156

1157

1158

1159

1160

1161

1162

1163

1164

1165

1166

1167

1168

1169

1170

1171

1172

1173

1174

1175

1176

1177

1178

1179

1180

1181

1182

1183

1184

1185

1186

1187

1188

Phi-3.5-vision Evaluation Instructions

User prompt: Judge the similarity of these images based on: - *Be sensitive to elastic transformations while evaluating images. For example, if the images are the same but have differing distortions due to elastic transformations, the similarity score should decrease. If the images are identical and have matching elastic transformations, the similarity score should remain high.*

The similarity score should reflect both the overall resemblance of the images and how well they satisfy the conditions. Identical images that do not meet the conditions should still score higher than completely unrelated images.

Provide a score on a scale of 1 to 10, with 1 being no similarity and 10 being identical images that satisfy all conditions. Respond strictly in this format:

Score: <1-10>

Reason: <reason for score>

Do not include additional text. What's your rating? "data1" "data2"

Phi-3.5-vision - Original Order**Model response:**

Score: 1

Reason: The images are highly distorted with elastic transformations, making it impossible to accurately compare the content.

Phi-3.5-vision - Reverse Order**Model response:**

Score: 10

Reason: The images are identical with no differences in content, color, or composition. They both depict the same scene with motorcycles and people in a bar setting, and the elastic transformations do not alter the image in any way.

B EXTENDED RELATED WORK

Using language models as automatic evaluators has become a somewhat common practice with popular approaches such as GPTSCORE and G-eval (Fu et al., 2023; Liu et al., 2023) being used to rank responses in the NLP domain. Due to that there has been a significant amount of recent work that has investigated the capabilities and limitations of using LLMs as judges (Thakur et al., 2024; Chiang & Lee, 2023; Murugadoss et al., 2024; Shankar et al., 2024). Chiang & Lee (2023) have shown that LLM evaluations are consistent and reproducible, making them suitable alternatives for human evaluation, they argue that these models inherent biases should prevent them using independently rather than *alongside* human experts. Furthermore, Zheng et al. (2023) reveal that large VLMs, e.g., GPT-4 Turbo, align well with human judgments and Thakur et al. (2024) further states that simpler models may still outperform GPT-4 Turbo in ranking tasks due to superior alignment metrics. Also, recent work assessed how humans can help LLMs evaluate better by testing different instruction

1188 types or designing tools that result in more balanced evaluations (Murugadoss et al., 2024; Shankar
 1189 et al., 2024).

1190 It is worth noting that known limitations of LLMs such as their lack of invariance to the order of
 1191 examples given in a prompt, which is a well studied issue of natural language models (Fang et al.,
 1192 2024), may render auto evaluation unreliable. Similarly, Berglund et al. (2023) show failure cases
 1193 where models trained on unidirectional relationships do not infer the reverse, indicating systemic
 1194 limitations even in state-of-the-art LLMs such as GPT-4 (as seen in Figure 1 and in Appendix A for
 1195 VLMs). Our main goal is to investigate the reliability of automated evaluation in the multimodal
 1196 context, by probing the models to compare data pairs.

1197 Namely, the evaluations we carry out focus on testing in multiple different ways how good VLMs
 1198 are when it comes to comparing data instances, such as whether VLMs prompted to compare are
 1199 symmetric or smooth for instance, and to what extent they can be controlled, i.e., instructed to pay
 1200 attention to or ignore certain features of the inputs. While the literature is more sparse regarding
 1201 testing VLMs in this setting, recent work has tested for something along those lines. Chen et al.
 1202 (2024a) for instance propose a benchmark for evaluating VLMs in multiple different scenarios,
 1203 including checking whether pairwise comparisons of responses to a query correlated with human
 1204 judgments. They concluded that although correlations are relatively high on comparison tasks, biases
 1205 and inconsistencies affect performance on pair scoring and batch ranking. Similarly, Awal et al.
 1206 (2024) introduced a synthetic dataset containing paired images that differ only along one feature (e.g.,
 1207 the color of an object). We seek to add to this branch of the literature by introducing a framework
 1208 where controlled experiments can be carried out to anticipate the performance of models when being
 1209 used as judges, and various different characteristics of automatic judges can be identified (e.g., how
 1210 smooth they are).

1211 Unlike the case of generative VLMs discussed above, discriminative visual language models such
 1212 as CLIP (Radford et al., 2021) are covered by a significant amount of recent work, and several
 1213 failure modes are well reported, mostly deriving from the fact this class of VLMs tends to behave
 1214 as bag-of-words models, focusing on nouns and ignoring relationships and semantics in their input
 1215 data (Yuksekgonul et al., 2023). For instance, CLIP was observed to struggle with spatial reasoning
 1216 (Kamath et al., 2023) and ignore negation (Alhamoud et al., 2025). On the other hand, fine-tuning
 1217 CLIP to reason about pairwise differences Sam et al. (2024) showed that discriminative VLMs can
 1218 improve on how well they manage to reason about pairwise differences if training is tailored for
 1219 enabling so, highlighting the benefits that being able to measure these skills may inform training
 1220 and improve models as a consequence. Ouali et al. (2024) showed that fine-tuning generative VLMs
 1221 to turn them into discriminative models results in improved image-retrieval from text, which aligns
 1222 with results we reported in Section C.5 showing a gap between open-sources VLMs and CLIP-style
 1223 encoders.

1224 C FULL RESULTS

1226 In this section, we provide the *MMScore* of all models on all the different splits of PB_{COCO}, PB_{IN100},
 1227 PB_{WU-II}, and PB_{WU-IT} in Tables 3, 4, 3, 4, 5, 6, and 7. We further report the coverage, the number of
 1228 times the VLMs give a valid output, of each model on our different proposed datasets.

1230 C.1 ALL ε -RELAXSYMFOR DIFFERENT ε S

1232 To show the ε -RelaxSym for different values of ε , we plot Figure 9 and show as ε gets higher, the
 1233 values go higher. However, some models such as the GPT4o models struggle with symmetry. Please
 1234 note that if $\varepsilon = 0$, it is the same as not having a threshold and hence calculating exact symmetry
 1235 rather than a relaxed version.

1237 C.2 VARIATIONS OF MMSCORE FORMULATION

1239 In this section, we examine how model rankings vary when Kendall’s Tau is replaced with other
 1240 correlation-based metrics, namely Normalized Mutual Information (NMI), Spearman’s rank correlation,
 1241 and Normalized Discounted Cumulative Gain (NDCG). Overall, we find that NMI, Spearman,
 and NDCG produce rankings consistent with those obtained using Kendall’s Tau. However, NDCG

1242
 1243 Table 3: Comparison of the *MMScore* metric ($\times 100$) of VLMs on PB_{COCO} and PB_{IN100} benchmarks
 1244 in the *sensitive* setting. Models are evaluated across multiple criteria: color jitter (CJ), elastic
 1245 transform (ET), gaussian blur (GB), perspective shift (PS), and rotation (R). Higher scores indicate
 1246 better performance.

Model	PB_{COCO}					PB_{IN100}				
	CJ	ET	GB	PS	R	CJ	ET	GB	PS	R
Chameleon-7B	00.37	00.34	00.19	00.31	00.60	00.38	00.26	00.31	00.50	00.52
LLaVA-OneVision-7B	36.51	44.05	38.57	43.80	41.41	37.05	49.89	40.00	46.01	49.30
Phi-3.5-vision	38.21	51.61	61.94	47.33	34.56	25.74	43.03	51.40	32.51	23.61
Pixtral-12B	37.67	56.25	54.32	49.53	36.80	30.75	52.30	51.94	46.04	40.76
InternVL2-1B	03.23	03.47	03.27	03.63	03.51	02.59	02.38	01.70	02.02	02.23
InternVL2-2B	23.89	32.76	34.32	31.53	24.76	18.32	34.02	33.35	28.17	23.35
InternVL2-4B	52.13	69.43	62.46	63.77	52.68	45.25	65.90	59.90	60.28	51.04
InternVL2-8B	51.58	62.80	62.35	60.27	54.80	47.94	60.18	58.60	56.66	53.00
InternVL2.5-1B	16.74	25.38	27.67	24.83	16.54	15.63	33.67	39.23	37.97	22.53
InternVL2.5-2B	12.48	19.58	25.26	18.33	13.84	17.27	38.28	39.21	31.23	21.45
InternVL2.5-4B	42.61	59.78	54.33	55.34	49.47	41.35	62.35	54.21	56.18	49.90
InternVL2.5-8B	54.51	73.37	78.31	63.17	60.71	51.76	77.10	76.40	60.40	55.30
MolmoE-1B	00.40	00.09	01.20	00.03	00.05	00.41	00.01	00.45	00.01	00.01
Molmo-7B-O	14.32	16.02	48.93	16.12	15.40	12.91	14.20	48.43	13.83	12.16
Molmo-7B-D	27.06	45.28	34.46	49.60	30.39	22.88	41.06	35.83	44.49	32.22
Qwen2-VL-2B	09.91	11.82	09.01	13.13	11.95	10.63	13.69	10.41	13.21	12.23
Qwen2-VL-7B	42.58	61.90	50.22	55.81	51.10	38.24	61.73	50.23	53.07	52.29
GPT-4o-mini-0718	49.98	65.97	58.29	53.23	53.60	47.06	67.06	56.43	49.97	52.59
GPT-4o-0513	50.96	65.54	61.67	56.69	56.71	48.55	65.68	57.48	54.11	55.00
GPT-4o-0806	42.26	60.58	56.62	50.13	53.63	40.35	60.66	52.65	49.62	49.77
GPT-4o-1120	51.31	63.50	61.35	57.84	57.16	50.88	66.55	58.14	56.25	55.52
Gemini-1.5-Flash	58.26	82.64	87.41	65.92	61.08	56.25	79.69	85.21	62.07	61.15
Gemini-1.5-Pro	53.33	87.86	89.56	74.92	71.04	51.19	91.36	92.98	71.56	74.22

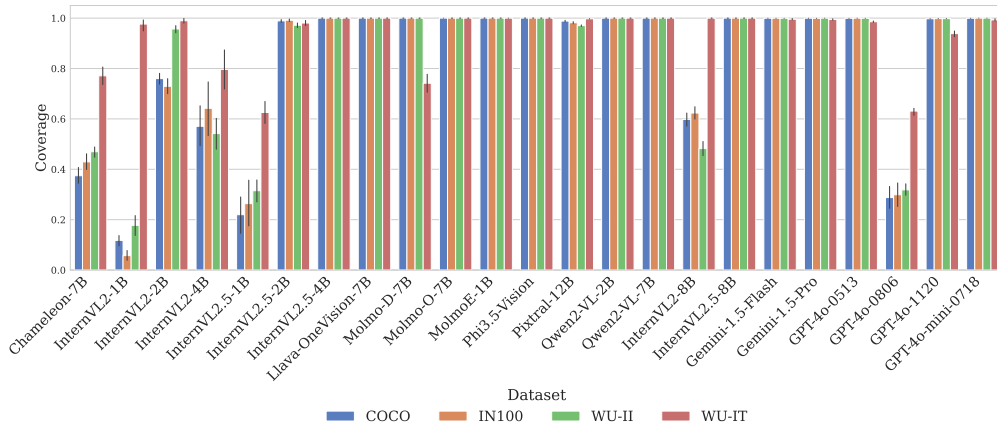


Figure 8: Coverage of each model.

1293 exhibits lower sensitivity, leading to flatter curves that are less informative for our setting. We attribute
 1294 this to the fact that NDCG was originally designed for retrieval systems, where the top-ranked items
 1295 dominate the evaluation, and thus the metric emphasizes alignment at the highest scores rather than
 capturing fine-grained differences across the full ranking. The results can be seen in Fig. 10.

1296

1297 Table 4: Comparison of the *MMScore* metric ($\times 100$) of VLMs on PB_{COCO} and PB_{IN100} benchmarks
1298 in the *invariant* setting. Models are evaluated across multiple criteria: color jitter (CJ), elastic
1299 transform (ET), gaussian blur (GB), perspective shift (PS), and rotation (R). Higher scores indicate
1300 better performance.

Model	PB_{COCO}					PB_{IN100}				
	CJ	ET	GB	PS	R	CJ	ET	GB	PS	R
Chameleon-7B	00.89	00.34	00.44	00.51	00.38	00.57	00.35	00.53	00.58	00.45
LLaVA-OneVision-7B	35.13	37.26	39.22	40.29	38.29	38.09	43.04	41.83	40.86	42.24
Phi-3.5-vision	49.41	40.19	42.93	55.03	47.90	45.88	33.79	39.72	50.41	39.46
Pixtral-12B	48.26	47.34	45.35	60.20	55.65	41.53	45.30	42.84	52.63	52.65
InternVL2-1B	02.69	01.76	02.71	02.00	02.69	01.39	00.82	01.22	00.90	01.40
InternVL2-2B	36.38	31.55	31.99	39.18	37.28	32.68	31.40	30.13	35.98	34.70
InternVL2-4B	59.44	55.47	51.35	59.61	59.02	51.74	52.77	49.60	54.63	53.11
InternVL2-8B	58.69	58.56	53.60	61.91	64.22	58.44	54.48	51.78	61.97	62.90
InternVL2.5-1B	21.39	18.59	21.65	23.19	22.86	22.52	14.63	24.34	22.76	19.24
InternVL2.5-2B	22.85	19.05	21.46	27.62	25.99	32.09	33.03	37.34	34.65	34.75
InternVL2.5-4B	56.24	47.41	43.93	53.71	55.28	61.80	50.50	47.33	51.58	58.56
InternVL2.5-8B	75.11	65.18	66.32	78.56	81.77	72.53	61.61	62.23	65.18	74.27
MolmoE-1B	00.10	00.11	00.06	00.02	00.00	00.02	00.11	00.10	00.07	00.25
Molmo-7B-O	26.86	34.58	33.46	34.70	24.55	25.04	30.81	38.52	32.79	27.65
Molmo-7B-D	47.20	45.02	43.02	50.54	48.64	45.01	45.83	45.47	49.25	40.87
Qwen2-VL-2B	09.55	09.10	10.21	12.65	08.83	09.02	09.61	10.01	14.97	09.33
Qwen2-VL-7B	50.52	51.80	52.70	54.50	53.29	47.86	49.73	51.18	51.55	50.67
GPT-4o-mini-0718	59.76	57.94	56.55	61.31	58.17	56.33	55.56	55.35	60.99	60.83
GPT-4o-0513	70.83	61.70	59.40	61.13	62.10	68.82	56.16	56.70	57.79	59.80
GPT-4o-0806	55.14	50.31	46.00	52.15	52.45	54.13	45.43	44.25	48.26	52.18
GPT-4o-1120	73.48	69.06	61.51	67.60	63.99	70.16	61.33	58.89	65.06	60.84
Gemini-1.5-Flash	72.11	67.81	68.17	71.88	78.31	70.32	65.94	66.58	69.10	74.77
Gemini-1.5-Pro	68.93	69.64	71.50	72.06	68.42	66.31	70.03	72.17	70.13	69.32

1325
1326 C.3 DIFFERENT VERSIONS OF SAME MODEL1327
1328 We further examine the effect of model capacity on the different metrics of PAIRBENCH. As seen in
1329 Figure 11, larger-capacity models tend to perform better across *MMScore*, ε -RelaxSym, and *Cont.*
1330 However, there are exceptions—for example, `InternVL2-4B` demonstrates greater controllability
1331 in rotation (R) and perspective shift (PS) compared to `InternVL2-8B`. Additionally, smoothness
1332 (*SM*) does not increase monotonically with model capacity. This suggests that stronger models may
1333 be more confident in their responses, leading to less diversity in their similarity scores compared to
1334 lower-capacity models.1335 On the other hand, Table 2 and Figure 13 show that *SM* correlates positively with model performance
1336 and other benchmarks, indicating that better models tend to produce smoother and more diverse
1337 outputs than weaker ones. Ultimately, we conclude that *SM* is not strictly a property of model
1338 performance but rather a characteristic of a VLM as a judge model that may be desirable (or not)
1339 depending on the use case.1340
1341 C.4 CORRELATIONS1342
1343 In this section, we further plot the correlations of the different metrics and show them in Figures 12,
1344 13, 13. As seen, all these metrics have positive correlations as seen in the scatter plots.1345
1346 C.5 ENCODERS VS VLMs1347
1348 For the image-image task, we explore how image encoders compare to VLMs on our metrics. To
1349 this end, three DINOv2 versions (`DINOv2-Base`, `DINOv2-Small`, and `DINOv2-Large`) and
the LAION- and OpenAI- CLIP-trained ViTs (base and large) are chosen to encode images. Since

1350

Table 5: Comparison of the *MMScore* metric ($\times 100$) of VLMs on PB_{WU-II} (subset A and B) benchmark in the *sensitive* setting. Models are evaluated across multiple criteria: spatial position (SP), spatial position and color jitter (SP-CJ), spatial position and elastic transform (SP-ET), spatial position and gaussian blur (SP-GB), spatial position and perspective shift (SP-PS), and spatial position and rotation (SP-R). Higher scores indicate better performance.

1355

1356

1357

1358

1359

1360

1361

1362

1363

1364

1365

1366

1367

1368

1369

1370

1371

1372

1373

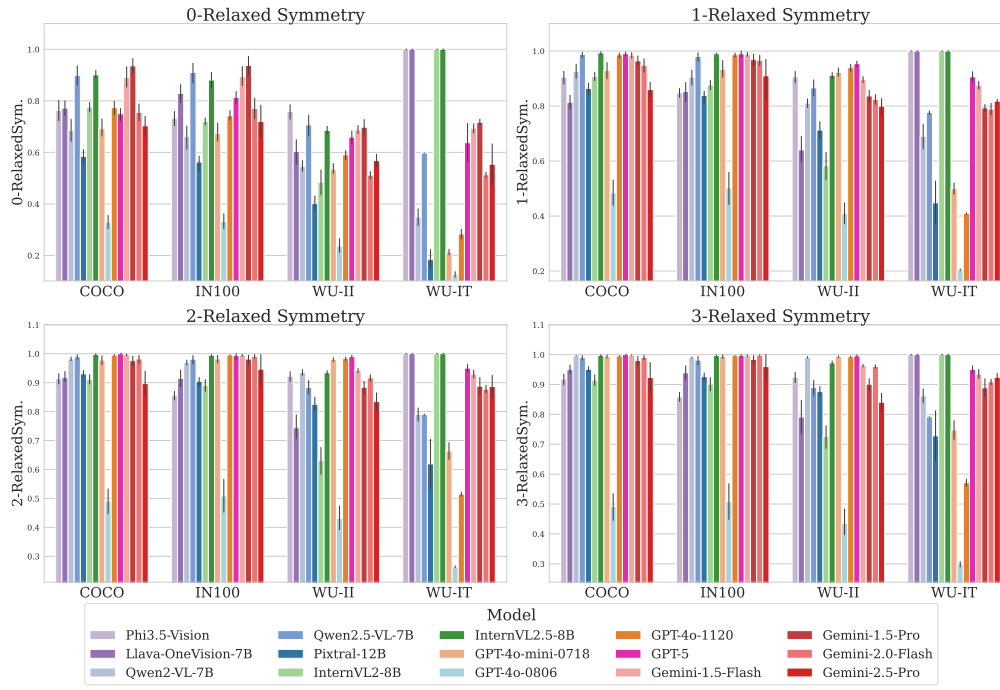
1374

1375

1376

1377

Model	PAIRBENCH _{WU_a}						PAIRBENCH _{WU_b}					
	SP	SP-CJ	SP-ET	SP-GB	SP-PS	SP-R	SP	SP-CJ	SP-ET	SP-GB	SP-PS	SP-R
Chameleon-7B	00.28	00.47	00.23	00.52	0.21	00.20	00.34	00.38	00.35	00.26	00.31	00.33
LLaVA-OneVision-7B	38.95	18.83	24.03	26.78	29.46	24.63	19.70	14.03	16.51	16.78	17.76	17.02
Phi-3.5-vision	23.44	08.46	15.70	19.41	13.34	10.83	15.38	12.98	18.91	20.19	11.69	17.06
Pixtral-12B	37.91	26.09	32.05	33.52	32.47	25.00	28.02	19.58	22.32	22.31	23.46	24.50
InternVL2-1B	00.44	00.98	00.79	00.65	00.30	00.28	00.20	-	-	00.41	01.18	00.90
InternVL2-2B	22.85	12.03	14.37	17.84	18.66	15.50	20.72	10.89	11.22	15.74	17.74	13.58
InternVL2-4B	46.89	27.91	36.67	43.03	44.27	27.76	44.89	27.77	33.35	38.12	42.23	36.16
InternVL2-8B	41.99	32.06	35.71	41.02	40.12	29.11	46.36	32.17	39.24	41.90	45.59	40.30
InternVL2.5-1B	25.50	14.16	21.32	15.69	21.49	16.30	24.77	16.16	21.10	19.95	27.89	21.47
InternVL2.5-2B	20.63	11.76	16.75	15.21	18.03	13.79	23.44	09.33	15.90	17.64	18.17	17.56
InternVL2.5-4B	46.15	32.74	39.05	39.24	42.28	32.94	47.93	33.75	40.23	39.82	44.07	42.57
InternVL2.5-8B	44.27	36.99	41.49	42.60	43.65	33.24	41.32	31.69	40.10	39.73	44.03	42.99
MolmoE-1B	00.47	01.03	00.00	00.03	00.14	00.01	00.32	00.36	00.01	00.04	00.04	00.09
Molmo-7B-O	15.94	09.90	11.32	15.38	12.92	12.01	15.15	08.40	11.39	11.33	13.60	12.50
Molmo-7B-D	23.82	17.75	20.41	18.40	22.21	17.81	26.74	18.37	19.55	18.77	18.19	22.21
Qwen2-VL-2B	02.26	01.76	02.58	02.15	03.17	01.68	00.88	00.44	00.73	00.37	00.72	00.82
Qwen2-VL-7B	41.95	29.47	36.32	39.93	40.33	34.11	42.80	28.75	31.42	37.27	39.76	36.25
GPT-4o-mini-0718	42.55	37.21	39.50	40.44	38.83	41.05	48.86	38.38	43.82	45.42	46.32	46.66
GPT-4o-0513	40.27	37.83	36.79	38.52	38.84	38.07	44.13	39.46	39.46	43.58	43.49	46.25
GPT-4o-0806	37.58	33.72	34.24	33.36	34.80	33.17	40.11	33.36	32.36	34.32	39.91	38.67
GPT-4o-1120	40.68	39.06	40.10	40.35	40.96	40.40	47.34	40.91	43.07	47.18	50.22	50.68
Gemini-1.5-Flash	44.63	38.85	37.19	39.11	35.76	34.57	49.91	40.29	42.92	46.34	47.01	46.40
Gemini-1.5-Pro	40.38	36.07	31.52	37.85	29.92	30.37	49.20	38.26	39.16	44.98	41.70	40.72

Figure 9: ε -RelaxSym for different ε s.

1399

1400

1401

1402

1403

feature controllability on image-encoders is limited to the image augmentation transformation (CJ, R, PS, GB, ET), we only compare image-encoders to VLMs on PB_{COCO} and PB_{IN100}.

1404
1405
1406
1407
1408
1409

Table 6: Comparison of the *MMScore* metric ($\times 100$) of VLMs on PBWU-II (subset A and B) benchmark in the *invariant* setting. Models are evaluated across multiple criteria: spatial position (SP), spatial position and color jitter (SP-CJ), spatial position and elastic transform (SP-ET), spatial position and gaussian blur (SP-GB), spatial position and perspective shift (SP-PS), and spatial position and rotation (SP-R). Higher scores indicate better performance.

1410
1411
1412
1413
1414
1415
1416
1417
1418
1419
1420
1421
1422
1423
1424
1425
1426
1427
1428

Model	PAIRBENCH _{WU_a}						PAIRBENCH _{WU_b}					
	SP	SP-CJ	SP-ET	SP-GB	SP-PS	SP-R	SP	SP-CJ	SP-ET	SP-GB	SP-PS	SP-R
Chameleon-7B	00.34	00.39	00.76	00.47	00.43	00.41	00.47	00.34	00.56	00.24	00.62	00.34
LLaVA-OneVision-7B	34.79	31.56	30.23	34.14	32.61	28.69	13.12	18.41	16.21	22.69	15.34	17.91
Phi-3.5-vision	23.66	32.84	18.90	21.36	30.14	19.10	19.88	36.74	22.40	23.47	30.04	26.06
Pixtral-12B	36.93	37.32	41.17	35.31	38.52	36.05	36.03	30.44	33.32	29.84	35.48	33.32
InternVL2-1B	00.57	01.08	02.02	01.02	00.89	00.37	00.65	00.81	00.96	00.50	00.56	00.54
InternVL2-2B	26.25	25.53	25.76	21.12	26.57	26.98	26.03	24.52	26.49	25.81	31.01	29.33
InternVL2-4B	39.33	40.23	37.80	42.25	43.10	34.57	51.43	41.55	45.96	50.20	54.94	50.34
InternVL2-8B	43.80	44.31	44.53	43.99	46.02	40.43	60.92	46.63	54.53	51.31	56.94	53.88
InternVL2.5-1B	12.82	13.84	09.34	07.24	12.91	16.93	19.87	24.92	19.36	17.94	22.66	30.60
InternVL2.5-2B	31.38	29.79	30.53	23.16	31.75	24.69	36.01	30.13	35.52	27.07	37.01	31.18
InternVL2.5-4B	48.79	53.58	54.52	48.09	52.78	46.46	50.51	48.71	53.45	52.03	53.77	50.12
InternVL2.5-8B	59.03	55.57	59.70	57.16	58.01	50.84	65.21	51.31	61.10	63.54	62.38	60.83
Molmo-E-1B	03.83	00.09	00.02	00.02	00.10	00.17	04.22	00.07	00.02	00.07	00.12	00.00
Molmo-7B-O	18.63	17.50	19.68	16.42	19.58	14.99	15.94	19.46	20.93	17.98	24.21	21.68
Molmo-7B-D	28.21	36.47	31.95	26.89	35.57	33.58	37.50	35.90	34.70	33.51	33.04	34.35
Qwen2-VL-2B	02.63	02.88	03.58	03.53	03.34	02.97	00.79	00.73	00.99	00.88	00.71	00.82
Qwen2-VL-7B	40.21	38.96	39.94	46.88	40.11	39.55	47.65	39.51	40.94	48.63	44.68	41.88
GPT-4o-mini-0718	47.60	48.33	51.04	46.15	48.86	43.75	57.50	49.19	51.38	53.76	55.82	54.07
GPT-4o-0513	52.39	51.58	48.78	47.11	47.50	52.68	61.59	59.77	58.08	60.95	61.53	63.74
GPT-4o-0806	50.94	47.21	46.52	42.90	45.84	52.50	62.75	54.23	53.20	51.19	58.50	57.21
GPT-4o-1120	57.47	56.25	54.40	56.11	54.40	57.93	65.91	62.22	63.93	67.96	66.86	68.10
Gemini-1.5-Flash	46.62	55.28	54.31	57.98	57.01	58.74	62.04	54.43	56.89	62.24	66.88	60.72
Gemini-1.5-Pro	38.07	35.08	35.05	36.11	33.21	33.23	56.43	42.24	43.74	48.41	50.40	45.83

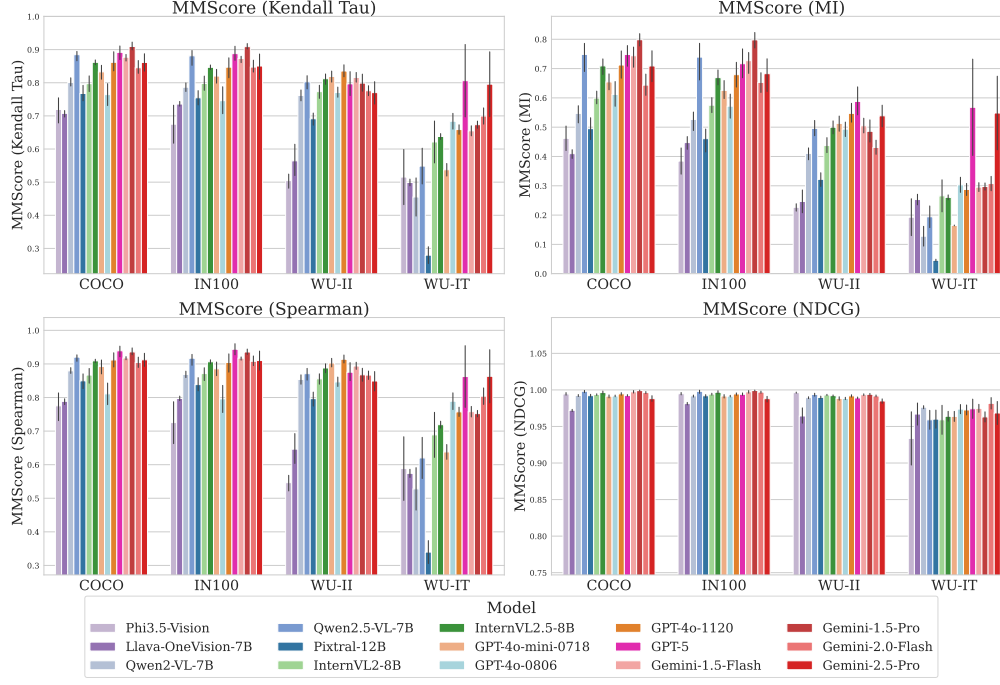
1429
1430
1431
1432
1433
1434
1435
1436
1437
1438
1439
1440
1441
1442
1443
1444
1445
1446
1447
1448
1449
1450
1451

Figure 10: Performance of models on PBWU-II if computed based on other formulations.

1455
1456
1457

To generate the similarity score of a given image-pair with an image-encoder, we compute the cosine similarity of the representation of each image and scale the scores between 1-10, and round them to the nearest integer. To generate the criteria-sensitive similarity score, we create the representations of the image-pair by simply using the representations output by the encoder for each image. On the

1458
 1459 Table 7: Comparison of the *MMScore* metric ($\times 100$) of VLMs on the $\text{PB}_{\text{WU-IT}}$ (Subset A and B)
 1460 benchmark in the *sensitive* and *invariant* settings. Models are evaluated across the spatial position
 1461 (SP) criterion. Higher scores indicate better performance.

Model	PAIRBENCH $_{WU_a}$		PAIRBENCH $_{WU_b}$	
	Sens.	Invar.	Sens.	Invar.
Chameleon-7B	00.25	00.34	00.23	00.47
LLaVA-OneVision-7B	23.35	22.78	27.38	25.98
Phi-3.5-vision	13.86	12.30	25.67	24.74
Pixtral-12B	05.14	05.04	03.27	04.58
InternVL2-1B	06.29	03.75	15.90	08.31
InternVL2-2B	17.07	14.26	24.46	16.49
InternVL2-4B	15.69	15.69	24.27	22.96
InternVL2-8B	22.40	19.27	29.45	31.46
InternVL2.5-1B	20.80	09.49	16.86	13.23
InternVL2.5-2B	15.36	11.15	19.69	18.42
InternVL2.5-4B	23.90	23.85	29.75	32.45
InternVL2.5-8B	24.16	25.55	24.00	28.22
MolmoE-1B	00.12	00.04	00.02	00.21
Molmo-7B-O	07.53	07.45	07.18	08.29
Molmo-7B-D	09.45	12.26	08.34	11.26
Qwen2-VL-2B	02.65	03.09	05.09	05.86
Qwen2-VL-7B	09.43	09.19	15.99	16.13
GPT-4o-mini-0718	16.18	16.14	16.18	15.30
GPT-4o-0513	11.49	20.48	12.63	20.98
GPT-4o-0806	20.27	31.80	22.97	36.56
GPT-4o-1120	18.97	31.91	20.57	34.99
Gemini-1.5-Flash	27.46	26.54	26.53	32.07
Gemini-1.5-Pro	26.89	27.16	28.57	29.23

1493 other hand, when generating the criteria-invariant score, where the criteria is a specific transformation
 1494 (T), we generate the representation of each image as the average of the representations of the encoder
 1495 for k versions of the image where random amounts of T are applied to the image. In our experiments,
 1496 we set $k = 5$.

1497 We report results in Figure 15. We see encoders do better than open-source VLMs most of the time
 1498 and are comparable to closed-source models (besides CJ). This shows although significantly smaller,
 1499 encoders can be at least as good as VLMs, enabling similarity scoring at a much lower cost. Also,
 1500 encoder-generated scores are trivially symmetric as well since the underlying cosine similarity is
 1501 symmetric. However, they lack in controllability as they are limited to image-only comparisons and
 1502 can only consider criteria that can be applied to the image using augmentations, i.e., spatial position
 1503 transform cannot be applied to images for encoders.

C.6 PROMPT DIVERSITY ANALYSIS

1507 To quantify the impact of prompt phrasing on model performance, we extend the visual analysis
 1508 presented in Figure 7 (see main text) with the detailed numerical results in Table 8. This table reports
 1509 the mean MMScore alongside the standard deviation across multiple prompt templates for each
 1510 evaluated model. The data reveals that sensitivity to prompting is not uniform; the standard deviation
 1511 varies considerably across different architectures. Furthermore, consistent with the trends observed in
 Figure 7, no single prompt template yields universally superior performance. These findings highlight

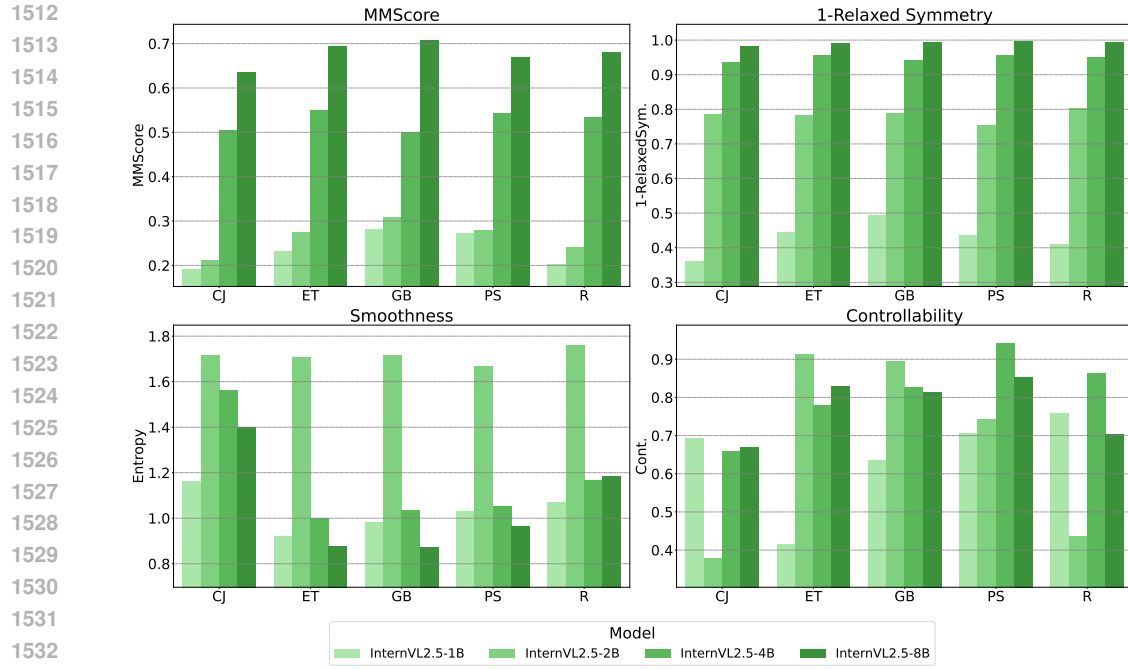


Figure 11: Aggregated PAIRBENCH metrics across different versions of InternVL2.5 models.

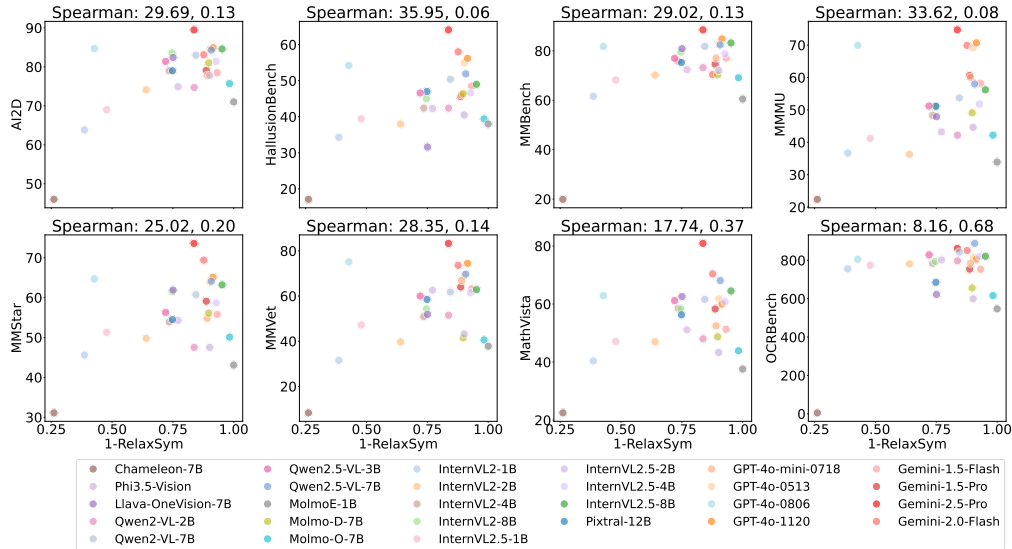


Figure 12: Other benchmarks versus PAIRBENCH on 1-RelaxSym.

the inherent variability in model responses and underscore the necessity of utilizing multiple prompt templates to mitigate selection bias and ensure a robust, fair comparison.

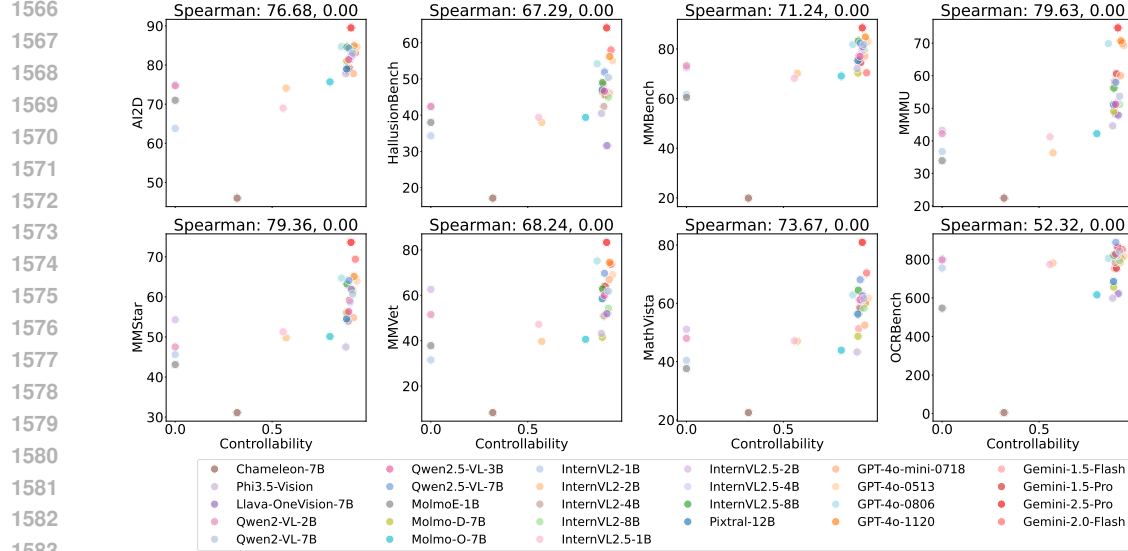
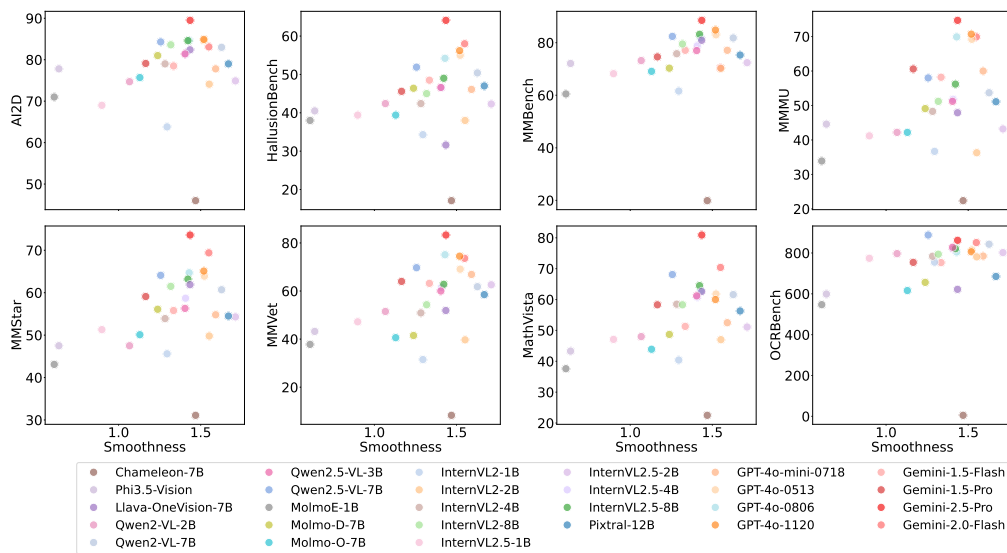
Figure 13: Other benchmarks versus *Cont* on PAIRBENCH.

Figure 14: Other benchmarks versus Smoothness (SM).

Table 8: Model performance across datasets for different prompt templates. Values are reported as Mean \pm Std.

Model	Dataset	MMScore (Kendall τ)	0-Relaxed Symmetry	Smoothness	Controllability
InternVL2-8B	COCO	80.69% \pm 1.02%	76.99% \pm 5.42%	1.09 \pm 0.05	89.96% \pm 2.77%
	IN100	80.72% \pm 1.38%	71.68% \pm 5.21%	1.16 \pm 0.03	89.30% \pm 3.00%
	WU-II	77.98% \pm 0.64%	47.27% \pm 8.46%	1.47 \pm 0.05	91.75% \pm 1.26%
	WU-IT	63.11% \pm 1.06%	100.00% \pm 0.00%	1.05 \pm 0.26	91.65% \pm 4.29%

Continued on next page

1620

Table 8 – continued from previous page

1621

1622

1623

Model	Dataset	MMScore (Kendall τ)	0-Relaxed Symmetry	Smoothness	Controllability
InternVL2.5-8B	COCO	86.21% \pm 0.89%	90.06% \pm 1.46%	0.99 \pm 0.03	84.41% \pm 0.10%
	IN100	84.71% \pm 0.64%	88.07% \pm 0.68%	1.11 \pm 0.03	83.30% \pm 1.25%
	WU-II	81.34% \pm 0.34%	68.58% \pm 1.18%	1.71 \pm 0.01	90.96% \pm 1.03%
	WU-IT	64.78% \pm 2.23%	100.00% \pm 0.00%	1.33 \pm 0.18	96.31% \pm 1.87%
Phi3.5-Vision	COCO	73.70% \pm 5.52%	76.27% \pm 4.47%	0.88 \pm 0.16	88.86% \pm 2.54%
	IN100	69.08% \pm 6.68%	73.31% \pm 2.95%	0.80 \pm 0.19	83.72% \pm 8.25%
	WU-II	52.81% \pm 9.40%	75.84% \pm 4.92%	0.29 \pm 0.25	74.99% \pm 7.75%
	WU-IT	52.80% \pm 2.13%	100.00% \pm 0.00%	0.97 \pm 0.26	95.03% \pm 2.24%
Pixtral-12B	COCO	78.57% \pm 3.67%	58.75% \pm 9.09%	1.36 \pm 0.13	87.06% \pm 2.13%
	IN100	77.56% \pm 3.34%	56.67% \pm 8.57%	1.38 \pm 0.11	86.86% \pm 2.52%
	WU-II	69.53% \pm 2.16%	40.26% \pm 3.63%	1.81 \pm 0.05	88.64% \pm 1.37%
	WU-IT	29.35% \pm 3.46%	18.29% \pm 1.90%	1.93 \pm 0.06	88.31% \pm 9.29%
Qwen2.5-VL-32B	COCO	83.40% \pm 1.92%	78.30% \pm 2.19%	1.08 \pm 0.05	87.69% \pm 1.61%
	IN100	82.16% \pm 1.21%	76.59% \pm 1.04%	1.17 \pm 0.06	87.07% \pm 1.08%
	WU-II	79.59% \pm 1.48%	63.66% \pm 1.96%	1.76 \pm 0.04	90.78% \pm 1.41%
	WU-IT	59.21% \pm 10.09%	26.81% \pm 24.50%	1.75 \pm 0.12	89.51% \pm 13.00%
Qwen2.5-VL-3B	COCO	73.55% \pm 1.37%	73.94% \pm 1.03%	1.40 \pm 0.06	84.87% \pm 3.40%
	IN100	75.07% \pm 2.79%	74.06% \pm 1.93%	1.31 \pm 0.07	81.89% \pm 2.19%
	WU-II	57.15% \pm 1.38%	42.48% \pm 2.51%	1.44 \pm 0.03	91.71% \pm 1.82%
	WU-IT	37.94% \pm 1.78%	51.49% \pm 8.77%	1.02 \pm 0.12	87.69% \pm 11.31%
Qwen2.5-VL-7B	COCO	88.56% \pm 0.31%	89.80% \pm 1.57%	0.99 \pm 0.04	87.52% \pm 1.10%
	IN100	88.22% \pm 0.36%	91.06% \pm 0.96%	0.96 \pm 0.04	85.68% \pm 1.48%
	WU-II	80.42% \pm 0.54%	70.66% \pm 1.77%	1.46 \pm 0.03	91.01% \pm 1.33%
	WU-IT	55.61% \pm 2.52%	59.81% \pm 3.50%	1.24 \pm 0.10	90.53% \pm 5.49%
Qwen2-VL-7B	COCO	80.83% \pm 1.79%	68.48% \pm 2.26%	1.43 \pm 0.05	91.14% \pm 1.43%
	IN100	80.23% \pm 2.15%	66.16% \pm 2.79%	1.38 \pm 0.03	92.24% \pm 2.34%
	WU-II	76.77% \pm 0.45%	54.57% \pm 2.18%	1.75 \pm 0.06	89.76% \pm 1.34%
	WU-IT	47.45% \pm 2.84%	34.87% \pm 3.40%	1.55 \pm 0.10	94.09% \pm 3.01%
GPT-4o-mini-0718	COCO	84.37% \pm 1.14%	69.27% \pm 2.91%	1.16 \pm 0.04	90.04% \pm 0.80%
	IN100	83.15% \pm 0.86%	67.28% \pm 2.67%	1.20 \pm 0.03	89.14% \pm 1.43%
	WU-II	82.45% \pm 0.39%	53.52% \pm 2.56%	1.81 \pm 0.03	92.53% \pm 1.10%
	WU-IT	53.77% \pm 6.44%	21.24% \pm 5.63%	2.11 \pm 0.05	95.72% \pm 2.78%
GPT-4o-0513	COCO	85.54% \pm 1.09%	73.40% \pm 1.51%	1.03 \pm 0.04	93.29% \pm 0.48%
	IN100	83.80% \pm 1.20%	70.65% \pm 1.64%	1.12 \pm 0.02	92.92% \pm 0.92%
	WU-II	82.75% \pm 0.28%	53.42% \pm 0.81%	1.78 \pm 0.01	94.73% \pm 0.49%
	WU-IT	52.47% \pm 4.86%	22.39% \pm 3.87%	1.99 \pm 0.08	88.03% \pm 7.59%
GPT-4o-0806	COCO	73.70% \pm 4.35%	24.38% \pm 18.29%	0.95 \pm 0.05	82.50% \pm 5.80%
	IN100	72.66% \pm 3.23%	24.73% \pm 18.83%	0.98 \pm 0.07	79.32% \pm 7.92%
	WU-II	74.34% \pm 5.40%	18.06% \pm 12.27%	1.62 \pm 0.08	85.94% \pm 4.17%
	WU-IT	69.06% \pm 0.91%	11.89% \pm 9.10%	2.00 \pm 0.09	85.32% \pm 7.09%
GPT-4o-1120	COCO	86.58% \pm 1.00%	77.32% \pm 1.93%	1.04 \pm 0.03	91.89% \pm 1.23%
	IN100	85.10% \pm 1.35%	74.24% \pm 2.39%	1.11 \pm 0.04	91.45% \pm 0.37%
	WU-II	83.82% \pm 0.33%	59.05% \pm 1.08%	1.77 \pm 0.03	93.85% \pm 0.61%
	WU-IT	65.78% \pm 2.80%	28.51% \pm 4.42%	1.92 \pm 0.09	79.85% \pm 5.87%

1673

Continued on next page

1674
1675 **Table 8 – continued from previous page**
1676
1677

Model	Dataset	MMScore (Kendall τ)	0-Relaxed Symmetry	Smoothness	Controllability
Gemini-1.5-Flash	COCO	87.75% \pm 0.63%	89.08% \pm 0.71%	0.87 \pm 0.02	85.41% \pm 1.08%
	IN100	87.40% \pm 0.27%	89.38% \pm 1.06%	0.91 \pm 0.05	83.86% \pm 1.01%
	WU-II	81.72% \pm 0.31%	68.75% \pm 1.43%	1.60 \pm 0.03	91.44% \pm 1.09%
	WU-IT	66.40% \pm 4.17%	69.39% \pm 3.51%	1.70 \pm 0.13	94.32% \pm 2.56%
Gemini-2.0-Flash	COCO	85.79% \pm 2.56%	75.57% \pm 8.20%	1.09 \pm 0.13	90.45% \pm 1.36%
	IN100	85.91% \pm 2.37%	76.99% \pm 6.52%	1.10 \pm 0.09	89.44% \pm 1.06%
	WU-II	78.08% \pm 0.96%	51.18% \pm 1.14%	1.81 \pm 0.03	93.78% \pm 1.02%
	WU-IT	71.12% \pm 2.08%	51.23% \pm 4.22%	1.71 \pm 0.05	95.29% \pm 2.50%
Gemini-1.5-Pro	COCO	90.97% \pm 0.50%	93.58% \pm 1.68%	0.76 \pm 0.04	83.31% \pm 1.47%
	IN100	90.99% \pm 0.79%	93.72% \pm 0.75%	0.76 \pm 0.02	83.49% \pm 1.42%
	WU-II	80.40% \pm 1.97%	69.79% \pm 2.64%	1.41 \pm 0.08	93.26% \pm 3.55%
	WU-IT	68.74% \pm 3.71%	71.81% \pm 6.28%	1.37 \pm 0.12	93.86% \pm 2.05%

1691
1692 **D PAIRBENCH DETAILS**1693 **D.1 DATASET CREATION**

1694
1695 The PAIRBENCH framework takes in a source dataset and creates augmented versions of the data
1696 to obtain data pairs to probe the evaluation skills of a model. In our instances, we use COCO (Lin
1697 et al., 2014), IN100 (Deng et al., 2009) and WhatsUp (Kamath et al., 2023) datasets as the source
1698 for the original data points. We utilize COCO and IN100 as image-only datasets and WhatsUp as
1699 an image-text dataset. We select 500 random images from each of COCO and IN100 and all the
1700 image-text pairs from both subsets provided by the WhatsUp dataset to be used in our instantiation of
1701 PAIRBENCH. Full details of our released datasets are given in Table 9.

1702
1703 To isolate the effect of different data characteristics on model performance, PAIRBENCH creates pairs
1704 of image-image and image-text data that are identical except for one or a few controlled features.
1705 The generated data consists of points from the original dataset paired with their transformed version.
1706 For COCO and IN100, we create a different control sample for each one of the transformations in
1707 $\{\text{color jitter, rotation, gaussian blur, perspective shift, elastic transformation}\}$, which defines the
1708 characteristic that differs between images. For the data from WhatsUp, we construct the data pairs by
1709 either only using the ‘spatial position’ transform, or ‘spatial position’ transform in addition to one of
1710 the previous five characteristics to additionally assess coupling effects. However, since transforms
1711 are not well-defined for texts, only ‘spatial position’ transform is applied for the image-text pairs.
1712 Note that the image-image pairs from WhatsUp are the most challenging since they all have at least
1713 the ‘spatial position’ transform, which is a well-known blind-spot of VLMs as shown by previous
1714 literature (Kamath et al., 2023; Wang et al., 2024a). As a result, we end up creating five image-image
1715 sub-datasets for each of COCO and IN100, six subsets for each of the two subsets of WhatsUp, using
1716 each of the transformations, and one image-text sub-dataset for each of the subsets of WhatsUp. The
1717 details of the transforms applied to each category are shown in Figure 3.

1718
1719 Next, for each original image, we construct three types of pairs: an identical, a transformed, and an
1720 irrelevant pair. In all three versions of these pairs, the first data point is the original (non-transformed)
1721 image. For the ‘identical’ pair, the second data point is another version of the image with 95% of its
1722 original size for the image-image pair and the correct caption for the image-text pair. The second data
1723 point in the ‘transformed’ pair is the original image (caption) with the transformation applied to it for
1724 the image-image (image-text) pair. Finally, the ‘irrelevant’ pair’s second data point is a transformed
1725 version of a random image (caption) from the rest of the dataset.

1726
1727 Equipped with the constructed control samples, PAIRBENCH prompts the VLM to score the similarity
1728 of each data pair based on a set of criteria. The criteria consists of the conditions indicating whether
1729 the model under examination should be ‘sensitive’ or ‘invariant’ to the transformations applied for
1730 that specific sub-dataset. These two settings (sensitive or invariant) measure how well each model

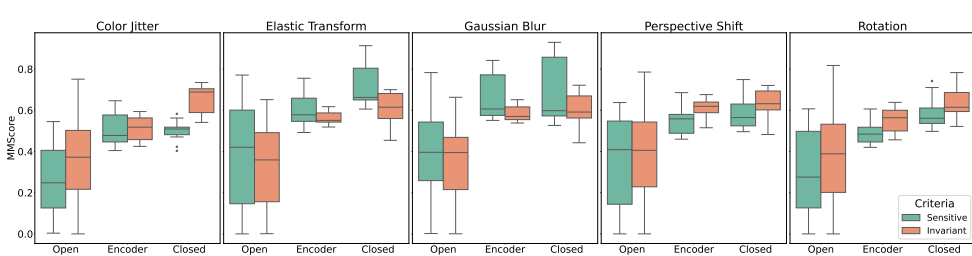


Figure 15: A simple vision encoder outperforms open-sourced VLMs and has on par performance with closed sourced models which are much more expensive, for image-image tasks (results combine PB_{COCO} and PB_{IN100}), and similar pattern is observed across different transformations.

Table 9: Information of different splits in PB_{COCO} , PB_{IN100} , $\text{PB}_{\text{WU-II}}$, and $\text{PB}_{\text{WU-IT}}$.

Modality	Source	Number of Selected	Splits	New Data Points / Total Data-Pair Comparisons
COCO		500	CJ	1000 / 3000
			R	1000 / 3000
			ET	1000 / 3000
			PS	1000 / 3000
			GB	1000 / 3000
IN100		500	CJ	1000 / 3000
			R	1000 / 3000
			ET	1000 / 3000
			PS	1000 / 3000
			GB	1000 / 3000
PB _{II}		418	SP	0 / 3344
			SP & CJ	1254 / 3344
			SP & R	1254 / 3344
			SP & ET	1254 / 3344
			SP & PS	1254 / 3344
			SP & GB	1254 / 3344
			SP	0 / 3264
PB _{IT}		408	SP & CJ	1224 / 3264
			SP & R	1224 / 3264
			SP & ET	1224 / 3264
			SP & PS	1224 / 3264
			SP & GB	1224 / 3264
In total	WhatsUp (subset A)	418	SP	1254 / 3344
			SP	1224 / 3264
In total	WhatsUp (Subset B)	408	SP	1224 / 3264
			SP	1224 / 3264
In total		1826	all splits	22390 / 69648

can recognize the differences between the data pair and follow the prompt’s criteria. If a model can successfully capture a specific feature, it will have no problem being variant or invariant to it; however, if it cannot detect it or has a bias towards a feature, it will favor being sensitive or invariant to that feature over its opposite. Using a human study, described in Appendix D.2, the ground-truth score of the ‘identical’ and ‘irrelevant’ pair are set to 10 and 1, respectively, in both ‘sensitive’ and ‘invariant’ settings. However, for the ‘transformed’ pair, based on the human study we set the score 10 in the ‘invariant’ version, and ‘6’ in the ‘sensitive’ version of the prompt. To make sure the performance gap between models is not merely a consequence of biased prompt wording, PAIRBENCH comes with five template prompts with different lengths and wordings but with the same semantic meaning, that are randomly selected for each data pair, to make sure the prompting does not affect the model’s performance. These prompt templates are reported in Appendix D.3.

Ultimately, we end up with 4 different datasets created by PAIRBENCH: PB_{COCO} , PB_{IN100} , $\text{PB}_{\text{WU-II}}$, and $\text{PB}_{\text{WU-IT}}$. PB_{COCO} and PB_{IN100} compare and score image-pairs and have 5 splits (Color Jitter

(CJ), Rotation (R), Gaussian Blur (GB), Perspective Shift (PS), and Elastic Transformation (ET). PB_{WU-II} consists of 2 subsets, each with 6 splits; one split with only the Spatial Position transform (SP), and the rest with SP combined with one of the previous five transformations (CJ, R, GB, PS, and ET). PB_{WU-IT} consists of only the SP split for each of the two subsets in the WhatsUp dataset. Details of each split in Appendix D.

1787

1788 D.2 HUMAN STUDY FOR GROUND TRUTH SCORES

1789

1790 To validate the alignment between our ground-truth scores and human perception, we conducted a
 1791 human study on **image-image** pairs from PB_{IN100}. We excluded image-text comparisons due to their
 1792 trivial nature for human judgment. For example, given an image showing a book to the left of a cap,
 1793 comparing it to the sentence “book left of cap” (identical), “book right of cap” (transformed), or “can
 1794 behind candle” (irrelevant) would result in nearly unanimous responses, offering limited insight.

1795 Our study involved 76 volunteer participants and covered 300 image pairs sampled across three trans-
 1796 formation types—color jitter, perspective shift, and rotation, under both “sensitive” and “invariant”
 1797 settings. Results from this evaluation led us to adjust the ground-truth score of transformed pairs
 1798 in the “sensitive” condition to 6 (on a 1–10 scale), as this better captured the perceptual similarity
 1799 reported by humans. Furthermore, the study confirmed that “identical” pairs consistently received the
 1800 highest scores, while “irrelevant” pairs received the lowest, supporting the validity of our scoring
 1801 protocol. A screenshot of the study can be seen in Figure 16 and the results are reported in Table 10.

1802 To assess the consistency of these judgments and account for potential subjectivity, we calculated
 1803 Krippendorff’s alpha Hayes & Krippendorff (2007) on the gathered human data following recent
 1804 methodologies Wiles et al. (2024); Hu et al. (2023). We obtained an alpha of 0.9396, which indicates
 1805 strong reliability in the conclusions drawn from the study. Additionally, we measured the leave-one-rater-
 1806 out noise ceiling using Spearman correlation and achieved an average of 0.9166. This further
 1807 confirms that the raters exhibit high agreement and that individual human judgments are highly
 1808 predictable from the average of the group.

1809

1810 Table 10: Human similarity scores (mean \pm std) across different transformation settings, which we
 1811 used to set our ground truth scores.

1812 Pair Type	1813 Colorjitter		1814 Perspective		1815 Rotate	
	1816 Sens	1817 Invar	1818 Sens	1819 Invar	1820 Sens	1821 Invar
1822 Identical	1823 9.8 ± 0.53	1824 9.95 ± 0.23	1825 9.82 ± 0.42	1826 9.9 ± 0.32	1827 10.0 ± 0.0	1828 9.89 ± 0.51
1829 Transformed	1830 5.5 ± 2.3	1831 9.68 ± 0.85	1832 6.89 ± 1.97	1833 9.06 ± 1.33	1834 6.31 ± 2.01	1835 9.36 ± 1.01
1836 Irrelevant	1837 1.35 ± 0.74	1838 1.42 ± 0.67	1839 1.33 ± 0.81	1840 1.61 ± 1.17	1841 1.27 ± 0.64	1842 1.23 ± 0.47

1843

1844

1845

1846

1847

1848

1849

1850

1851

1852

1853

1854

1855

1856

1857

1858

1859

1860

1861

1862

1863

1864

1865

1866

1836

1837

1838

1839

1840

1841

1842

1843

1844

1845

1846

1847

1848

1849

1850

1851

1852

1853

1854

1855

1856

1857

1858

1859

1860

1861

1862

1863

1864

1865

1866

1867

1868

1869

1870

1871

1872

1873

1874

1875

1876

1877

1878

1879

1880

1881

1882

1883

1884

1885

1886

1887

1888

1889

PairBench Human Evaluation

User ID: testing

Do not refresh page while taking the survey!

Sample 1 of 30

Instruction:

Score the similarity of the two images on a scale of 1 (least similar) to 10 (completely similar) given the condition[s] below:

- Be invariant to rotations while evaluating images. For example, if one image is a rotated version of the other, the similarity score should remain high. If the images are different, the similarity score should decrease regardless of their orientation.

Note: *Identical images that do not meet the condition[s] should score higher than irrelevant images.*

⚡ Similarity conditions for this pair:

- *Rotational difference DOES NOT decrease the score.*

If the images are different, decrease the score regardless.



Image 1



Image 2

Select your score (1 = least similarity, 10 = highest similarity):

1

2

3

4

5

6

7

8

9

10

[Restart with new samples](#)

Progress: 1 / 30

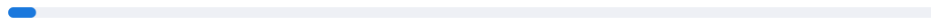


Figure 16: Example screenshot of the platform used consisting of the type of questions that participants were asked during the study. In the current sample, although both images depict birds, given that they are not a transformation (e.g., rotation) of each other, they represent an irrelevant pair; so the ground truth score would be the minimum score.

1890 D.3 PROMPT TEMPLATES FOR DIFFERENT PAIRBENCH DATASETS
1891
18921893 We provide the 5 different templates that we choose at random for each data pair for the image-image
1894 and image-text prompts. The following are the templates we utilize for PB_{COCO} and PB_{IN100} , and
1895 $\text{PB}_{\text{WU-II}}$, i.e., the image-image pairs.
1896
1897
18981899 **Image-Image Prompt Template V1**
19001901 *User prompt:* You are tasked with evaluating the similarity between two images while paying
1902 attention to the following conditions: {conditions}. Your goal is to judge the similarity
1903 of the images overall, where satisfying the conditions increases the similarity score. If the
1904 images are identical but fail to meet any of the conditions, they should still receive a higher
1905 score than completely unrelated images. Provide a similarity score on a scale from 1 to 10,
1906 where 1 represents entirely dissimilar images and 10 represents identical images that satisfy
1907 all conditions. Ensure your response is strictly in the following format:
19081909 **Score:** <1-10>
1910 **Reason:** <reason for score>
19111912 Do not include anything else in your response. What score would you assign to this pair of
1913 images? "data1" "data2".
1914
19151916 **Image-Image Prompt Template V2**
19171918 *User prompt:* As a similarity evaluator, your responsibility is to assess the similarity of
1919 the given images while considering these conditions: {conditions}. The similarity
1920 score should reflect both how well the images align with the conditions and their overall
1921 resemblance. Images that are identical but do not meet the conditions should receive a
1922 moderate score, while completely unrelated images should receive the lowest score. Provide
1923 your score on a scale of 1 to 10, with 10 being identical images that fully meet the conditions.
1924 Ensure your response is in the following format:
19251926 **Score:** <1-10>
1927 **Reason:** <reason for score>
19281929 Provide nothing else. What is your score? "data1" "data2"
1930
19311932 **Image-Image Prompt Template V3**
19331934 *User prompt:* Evaluate the similarity of the images based on the following conditions:
1935 {conditions}. The score should take into account how well the images align with these
1936 conditions, as well as their overall resemblance. Even if the images are identical but fail to
1937 meet the conditions, they should still receive a higher score than completely different images.
1938 Provide a score from 1 to 10, where 1 indicates no similarity and 10 indicates identical images
1939 that fully satisfy the conditions. Respond only in this format:
19401941 **Score:** <1-10>
1942 **Reason:** <reason for score>
19431944 Nothing else should be included. What score would you give? "data1" "data2"
1945

1944

1945

1946

1947

1948

1949

1950

1951

1952

1953

1954

1955

1956

1957

Image-Image Prompt Template V4

User prompt: Judge the similarity of these images based on: {conditions}. The similarity score should reflect both the overall resemblance of the images and how well they satisfy the conditions. Identical images that do not meet the conditions should still score higher than completely unrelated images. Provide a score on a scale of 1 to 10, with 1 being no similarity and 10 being identical images that satisfy all conditions. Respond strictly in this format:

Score: <1-10>

Reason: <reason for score>

Do not include additional text. What's your rating? "data1" "data2"

Image-Image Prompt Template V5

User prompt: Rate the similarity of these images on a scale of 1 to 10 while considering {conditions}. The score should account for both how well the images satisfy the conditions and their overall resemblance. If the images are identical but do not meet the conditions, they should still score higher than unrelated images. Your response must follow this exact format:

Score: <1-10>

Reason: <reason for score>

Provide nothing else. What's your score? "data1" "data2"

And these are the image-text versions for PBWU-IT:

Image-Text Prompt Template V1

User prompt: You are assigned the task of determining how accurately a text description represents an image of two objects. Pay special attention to the following conditions: {conditions}. Your goal is to assess the alignment between the image and the text, where adherence to the conditions increases the similarity score. If the text partially describes the image but fails to meet specific conditions, it should still score higher than a text entirely unrelated to the image. Assign a similarity score on a scale from 1 to 10, where 1 signifies no correlation, and 10 denotes perfect alignment satisfying all conditions. The data pair (text and image) will follow this prompt. Respond strictly in the following format:

Score: <1-10>

Reason: <reason for score>

What score would you assign to this text-image pair? "data1" "data2".

Image-Text Prompt Template V2

User prompt: Figure out how well this image matches the description provided. The image shows two objects, and the text is meant to describe how they're arranged. Look at these specific conditions: {conditions}. If the text captures some parts of the image but misses others, it should still get a better score than something totally off. Score this match on a scale of 1 to 10, where 1 means there's no match and 10 means the description nails it and matches every condition perfectly. The text and image will follow this prompt. Answer in this format only:

Score: <1-10>

Reason: <reason for score>

What's your score? "data1" "data2".

1998

1999

2000

2001

2002

2003

2004

2005

2006

2007

2008

2009

2010

2011

2012

2013

2014

2015

2016

2017

2018

2019

2020

2021

2022

2023

2024

2025

2026

2027

2028

2029

2030

2031

2032

2033

2034

2035

2036

2037

2038

2039

2040

2041

2042

2043

2044

2045

2046

2047

2048

2049

2050

2051

Image-Text Prompt Template V3

User prompt: Evaluate the degree to which a text description accurately represents an image featuring two objects, taking into account the following conditions: {conditions}. Assign a score based on how well the image-text pair matches, where: - A perfect description that satisfies all conditions scores 10. - Texts that partially align with the image but fail to meet conditions should still score higher than completely unrelated ones. The data pair will follow this prompt. Provide your score on a scale of 1 to 10 using the exact format below:

Score: <1-10>
Reason: <reason for score>

What score would you give? "data1" "data2".

Image-Text Prompt Template V4

User prompt: You are tasked with reviewing how well a text description aligns with an image of two objects. The score should reflect not only the accuracy of the alignment but also how well the description satisfies the following conditions: {conditions}. Even if the text description captures some parts of the image while failing the conditions, it should still receive a higher score than a completely irrelevant description. The text and image will be provided below. Assign a score on a 1 to 10 scale, where 1 is no similarity and 10 is perfect alignment that meets all conditions. Answer only in this format:

Score: <1-10>
Reason: <reason for score>

What score would you assign? "data1" "data2".

Image-Text Prompt Template V5

User prompt: Assess the degree to which a text description corresponds to an image of two objects, taking into account the following conditions: {conditions}. The scoring should reflect: - A perfect alignment with the image that satisfies all conditions merits a score of 10. - Descriptions that partially match the image but fail to meet certain conditions should still receive a higher score than entirely unrelated descriptions. - A score of 1 should be reserved for cases where no correlation exists between the text and the image. The text and image pair will be provided below. Provide your evaluation using the following format:

Score: <1-10>
Reason: <reason for score>

What score would you assign? "data1" "data2".

E LLM USAGE

LLMs were used in this work as assistive tools, but did not contribute as co-authors. Their usage was limited to the following areas:

- Benchmark Evaluations:** Since PairBench is a benchmark paper, we employed LLMs as evaluators to score and rank model outputs under different conditions.
- Automation of L^AT_EX Tables and Editing:** LLMs were used to automate the generation of L^AT_EX tables summarizing results and ablations, as well as for minor editing tasks (e.g., reformatting sections, ensuring consistent style).
- Writing Assistance:** LLMs assisted with grammar checking, improving sentence clarity, and smoothing transitions between sections. All scientific claims, analyses, and conclusions were written and verified by the human authors.